The Kregnes moraine in Gauldalen, west-central Norway: anatomy of a Younger Dryas proglacial delta in a palaeofjord basin*

W. NEMEC, IDA LØNNE AND LARS H. BLIKRA

BOREAS

Nemec, W., Lønne, I. & Blikra, L. H. 1999 (December): The Kregnes moraine in Gauldalen, west-central Norway: anatomy of a Younger Dryas proglacial delta in a palaeofjord basin. *Boreas,* Vol. 28, pp. 454–476. Oslo. ISSN 0300-9483.

The Kregnes "moraine" ridge in Gauldalen, a north-trending valley south of Trondheim, is a Gilbert-type delta formed at a Younger Dryas glacier terminus. The gravelly delta consists of a north-dipping foreset, 150 m thick, comprised of turbidites, debrisflow beds and debrisfall deposits. The bottomset consists of turbiditic sand and mud layers. The topset, 2–3 m thick, is a braided-river alluvium with local beach deposits, matching the marine limit of 175 m a.s.l. The fjord-wide delta front had an extent of 3 km and prograded over a distance of 1.5 km, in probably less than 100 years, with the delta toe climbing by 50 m against the basin's rapidly aggrading muddy floor. The delta advanced through the alternating episodes of its toe aggradation and progradation, related to the increases and decreases of the delta-slope gradient. Slope steepening led to intense sediment sloughing by chutes and occasional large-scale failures. The fjord's wave fetch was low and the wave base no deeper than 1.5–2 m, but strong storm waves occasionally reworked the delta front to a depth of 6 m. Glacitectonic deformation was limited to the system's upfjord end. Allostratigraphic analysis suggests that the proglacial system commenced its development as an ice-contact submarine fan that was deformed, quickly aggraded to the sea surface and turned into an ice-contact delta, which further evolved into the large glaciofluvial delta. The Kregnes ridge represents an episode of the ice-front re-advance due to climatic deterioration and is tentatively correlated with the Hoklingen substage.

W. Nemec, Geological Institute, University of Bergen, N-5007 Bergen, Norway. E-mail: Wojtek.Nemec@geol.uib.no; Ida Lønne, The University Courses on Svalbard (UNIS), PO Box 156, N-9170 Longyearbyen, Norway; Lars H. Blikra, The Geological Survey of Norway, PO Box 3006, N-7491 Trondheim, Norway; *received 6th October 1988, accepted 21st April 1999*

The ice-front deposits of the Younger Dryas episode of pronounced climatic cooling and glacial re-advance (11 000–10 000 BP) are recognizable as series of "moraine" ridges at the whole rim of Scandinavia and its eastern surroundings (Lundqvist *et al.* 1995). The nature of these topographic ridges varies (Lønne 1995), but they are often the most distinct glacial landforms in the region. Much work has been done on the geomorphological mapping, dating and correlation of these features (see review by Lundqvist & Saarnisto 1995; Andersen *et al.* 1995a), and the more recent studies have demonstrated that the sedimentary ridges bear the important record of the local ice-front behaviour and are crucial sources of information for the reconstruction of the ice-sheet dynamics (Powell 1981; Boulton 1986; Lønne 1993, 1995, 1997a, b). The present case study contributes to our understanding of the Younger Dryas history of the Scandinavian ice-sheet and the origin of the "moraine" ridges.

The paper describes an ice-front ridge at Kregnes in Gauldalen, west-central Norway (Fig. 1), whose origin and depositional history are discussed on the basis of a detailed sedimentological study and allostratigraphic facies analysis. The Kregnes "moraine" is interpreted to be a glaciomarine Gilbert-type delta, the development of which was controlled by the ice-front position, fjord confinement and relative sea level. Radiocarbon dates on marine fauna indicate that the deltaic ridge was formed in the Younger Dryas. The study focuses on the depositional processes and facies anatomy of this gravelly proglacial delta and sheds new light on the Younger Dryas ice-front dynamics and the climatic and environmental changes in the Gauldalen palaeofjord.

Local deglaciation and depositional setting

The history of the Late Weichselian deglaciation in the surroundings of Trondheim has been reconstructed by Reite (1983, 1985, 1994). The sedimentation area south of Trondheim includes two north-trending valleys, now occupied by the rivers Gaula and Nidelva (Fig. 1), which have acted as glaciated fjords during the southwestward retreat of the ice-sheet from the coastal zone at the end of the last glacial. The Late Weichselian marine limit in the area is at an altitude of *c.* 175 m,

* This paper is the result of an NFKS/NGU workshop held on 25–28 May 1993 and attended by the following researchers: B. Bergstrøm, L. H. Blikra (technical organizer), E. Larsen, T. Lauritsen, I. Lønne, E. Mauring, A. Misund, W. Nemec (leader), L. Olsen, D. Ottesen, A. J. Reite, H. Sveian and M. Thoresen. While each member of the group contributed to the field study, the three authors are solely responsible for the present report.

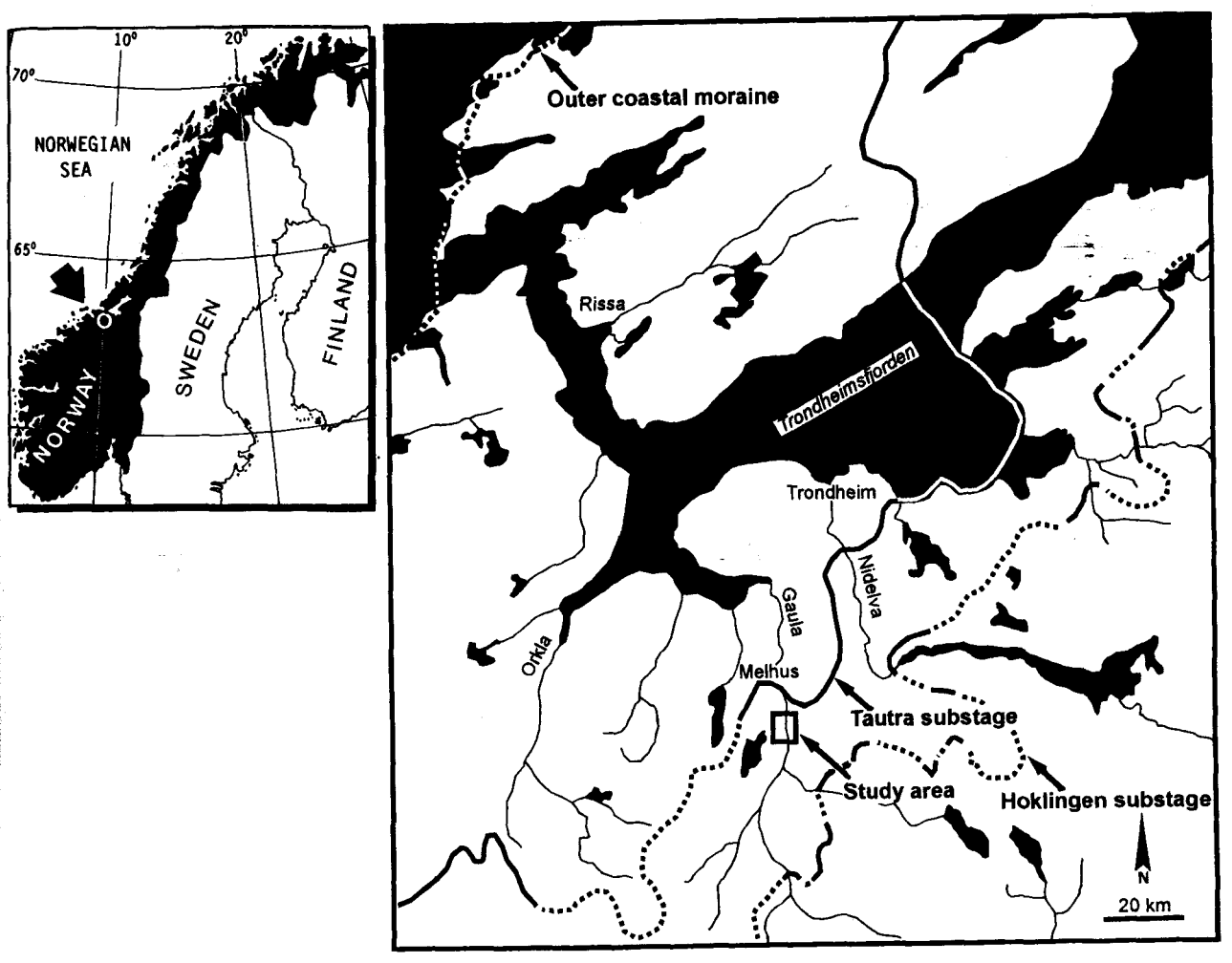

Fig. 1. Locality maps showing the study area in Gauldalen and the reconstructed ice-front positions in the outer coastal zone (12 400–12 300 BP) and the Tautra (10 800–10 500 BP) and Hoklingen (10 400–10 300 BP) substages of the Younger Dryas (after Reite 1985).

marked by marine beach terraces and delta topset deposits. The palaeofjords are overdeepened valleys, scoured in the metamorphic sedimentary/volcanic rocks of Cambro-Silurian age (Wolff 1979), with a relief of 800–1000 m and the deepest floor *c.* 300–400 m below the present-day sea level. The valleys have been filled with a succession of Late Weichselian glaciomarine to marine deposits, reaching a thickness of 200 m (estimated from seismic data; Reite 1983). The present study focuses on the western valley, Gauldalen (Fig. 1).

Reite (1994) has recognized three series of correlative ice-margin features, thought to represent distinct stillstand/re-advance positions of the retreating ice front, and ascribed them to the outer coastal stage (12 400–12 300 BP) and the Tautra (10 800–10 500 BP) and Hoklingen (10 400–10 300 BP) substages of the Younger Dryas glaciation (Fig. 1; see also review by Andersen *et al.* 1995b). The Kregnes moraine in Gauldalen is located between the moraine ridges interpreted by Reite (1994) to represent the latter two ice-front positions (Fig. 1).

The moraine ridge near Melhus (Fig. 2A) reaches an altitude of 120 m and consists of a large-scale gravelly foreset overlain by muddy glaciomarine to marine deposits. We interpret this ridge to be an ice-contact submarine fan (*sensu* Lønne 1995) deposited at the terminus of a re-advancing glacier. The moraine ridge at Kregnes, 5 km to the south (Fig. 2A), reaches the altitude of the marine limit and consists of a large-scale gravelly foreset overlain by fluvial topset deposits. We interpret this younger, upvalley ridge as a proglacial Gilbert-type delta developed at the front of a grounded glacier. The southern margin of the delta is a topographic escarpment (Fig. 2B), where the only evidence of glacitectonic deformation has been recognized (ice-contact zone). The delta originally occupied the full width of the fjord, but has subsequently been traversed and deeply dissected by the Gaula river. The whole

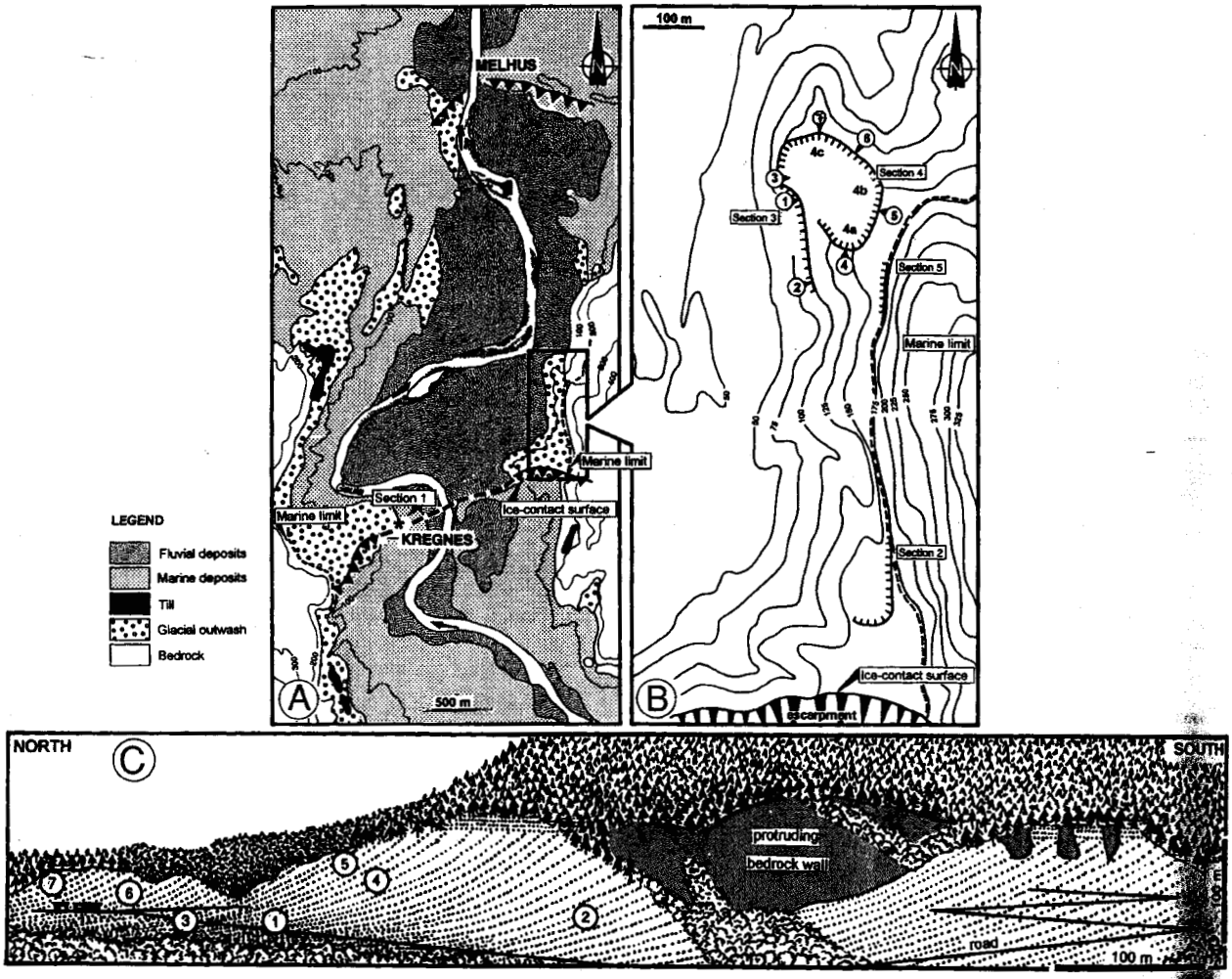

Fig. 2. □A. Detailed geological map of the studied part of Gauldalen (after Reite 1983), showing the ice-front positions near Melhus and Kregnes and the location of outcrop section 1. □B. Topographic map of the eastern part of the Kregnes ridge, showing the locations of sections 2–5 and logs 1–7. □C. Sketch of the Kregnes delta in outcrop sections 2–5, with approximate locations of logs 1–7.

middle part of the delta has been eroded by the river's wandering channel, with the delta relicts preserved as prominent terraces on both sides of Gauldalen (Fig. 2A). Our detailed observations are from an outcrop section on the valley's western side (section 1 in Fig. 2A) and four gravel-pit sections on the eastern side (sections 2–5 in Fig. 2B). The sedimentological logs are mainly from sections 3 and 4 (see localities 1–7 in Fig. 2B, C).

The Kregnes delta

The sedimentary succession at Kregnes is up to 150 m thick and consists of well-bedded sand and gravel. The deposits form a giant coarsening-upward foreset overlain erosively by a horizontally bedded topset, *c.* 3 m thick (Fig. 2C), whose altitude matches the local marine limit of 175 m a.s.l. The corresponding bottomset consists of subhorizontally bedded silt and sand, but its outcrops are inaccessible for closer examination. The large-scale tripartite structure of the succession indicates a Gilbert-type delta.

The delta foreset beds are dipping northwards and the delta toe rises in that direction (Fig. 2C), apparently "climbing" against the muddy prodeltaic deposits of the palaeofjord basin. The foreset thickness decreases from 150 m in section 1 (Fig. 2A) to little more than 100 m in the northern part of section 4 (Fig. 2B), which means that the prodelta zone has aggraded by *c.* 50 m during the delta-front progradation over a distance of *c.* 1.5 km.

The ensuing description and genetic interpretation of the delta's sedimentary facies focuses on the foreset and topset deposits.

Foreset facies

The foreset beds have a large-scale tangential geometry (Fig. 2C), with the maximum dip angle of 30–33° and a mean inclination of 18–20°. The beds in the foreset toe are generally inclined at less than 10°. The proportion of gravelly deposits in the foreset varies, and its youngest part is relatively rich in gravel. The foreset deposits represent the delta's avalanching subaqueous slope and include the following genetic facies: (1) turbidites, (2) debrisflow deposits and (2) debrisfall gravel. These are described and discussed below. The terminology for gravel characteristics is after Walker (1975); the fabric notation uses symbols *a* and *b* for the clast long and intermediate axes, with indices (t) and (p) denoting axis orientation transverse or parallel to flow direction, and index (i) denoting axis imbrication. The notation of turbidites, T*abc*, refers to the Bouma divisions. All sample dates are in radiocarbon years.

Turbidites. – Deposits interpreted as turbidites predominate in the toe part of the delta foreset; they constitute 40–60 vol.% of its mid-slope part and are relatively rare in the upper part. These are beds of pebble gravel and sand that show normal grading and/or stratification, which means evidence of deposition from a turbulent flow. According to the terminology of Lowe (1982), turbidites that show stratification directly from the base upwards, indicating fully tractional deposition, are classified as the deposits of low-density turbidity currents (LDTCs), whereas beds that are merely graded, with or without a stratified upper part, are classified as the deposits of high-density turbidity currents (HDTCs).

The HDTC deposits are discrete beds of pebble gravel and/or coarse sand, mainly 5–30 cm thick (Fig. 3A; logs 5 and 6 in Figs. 4 and 5), but reaching 50–65 cm (see the upper half of log 2 in Fig. 6). In terms of the conventional Bouma divisions, these beds can be classified as turbidites T*a* and T*ab*. They are attributed to surge-like turbidity currents, triggered by the release of limited sediment volumes by discrete failures of the delta's upper slope and/or brink zone. The finer-grained, low-density parts of these currents have apparently bypassed the delta slope and deposited their load in the delta toe and prodelta zone. The occasional presence of outsized pebbles at the gravel-sand transition in a HDTC deposit (Fig. 3A) can be attributed to the transport mechanism suggested by Postma *et al.* (1988), but the common occurrences of scattered cobbles at the bed boundaries are thought to represent coeval debrisfall processes (discussed further below). The turbidites occasionally show an unusual top division, composed of a homogeneous sand with large floating pebbles, coarser than the basal gravel of the overlying bed (Fig. 7A). We infer that some of the HDTCs, when arriving on a sandy lower slope, have sheared and liquefied the substratum, such that the current's coarse bedload became effectively entrapped by the latter (Fig. 7B).

The LDTC beds, in contrast, are commonly as much as 70–200 cm in thickness and show essentially one type of stratification, but with common grain-size fluctuations and little obvious grading. Planar parallel-stratified turbidites T*b*, composed of fine gravel or pebbly sand, predominate in the middle/lower part of the delta slope (see logs 2, 3, 5 and 6 in Figs. 6, 8, 4 and 5, respectively), whereas sandy turbidites T*c*, with mainly climbing-ripple cross-lamination (Fig. 3B, C), prevail in the toe part of the delta foreset, where their composite, amalgamated units often attain a thickness of a few metres (see log 1 in Fig. 6). The beds are attributed to sustained, relatively long-duration turbidity currents, probably related to the episodes of a retrogressive slumping of the delta front or generated directly by the river effluent (Bornhold & Prior 1990; Nemec 1990). Debrisfall products, in the form of isolated cobbles or lenticular intercalations of coarse gravel, are commonly associated with turbidites T*b* (see logs 3, 5 and 6 in Figs. 8, 4 and 5), but seldom with turbidites T*c* (see log 1 in Fig. 6). The large clasts, when tumbling downslope, were likely affected by the coeval upper-stage turbidity current and may have rolled for a short distance in its bedload traction. The transport competence of the lower flow-regime currents was much more limited.

In the toe part of the delta foreset, the amalgamated packages of fine- to medium-grained sandy turbidites T*c*, often intercalated with thin turbidites T*(a)b*, form coarsening-upward accumulations (see the lower part of log 1 in Fig. 6) whose convex-upward tops and "compensational" offset stacking suggest a series of depositional lobes, similar to those described by Postma & Cruickshank (1988). The turbiditic lobes have apparently coalesced with one another into an aggradational ramp, overlain by a series of multistorey, turbidite-filled channels (see Fig. 9 and the upper part of log 1 in Fig. 6), interpreted to be the lower reaches of delta-slope chutes. Several turbidite-filled chutes, or possibly gullies related to localized slope failures (Nemec 1990), have been recognized in the higher part of the delta foreset, where their infill is coarser grained and often more complex (see example in Fig. 10). Accordingly, the delta-toe sand lobes are thought to be chute-mouth deposits, whose accumulation was likely instigated by the hydraulic-jump conditions of the slope-base break. The sustained LDTCs were probably generated by a semicontinuous, retrogressive slumping of river mouth bars, advancing onto the steep delta slope. The chutes were apparently shifting their position on the delta slope (Fig. 9), but unable to extend their course further into the slope base/prodelta zone until the hydraulic jump had effectively been cancelled by the ramp aggradation.

Thick turbidites T*(a)b*, related to sustained currents, are locally observed to have formed "backsets", or sets

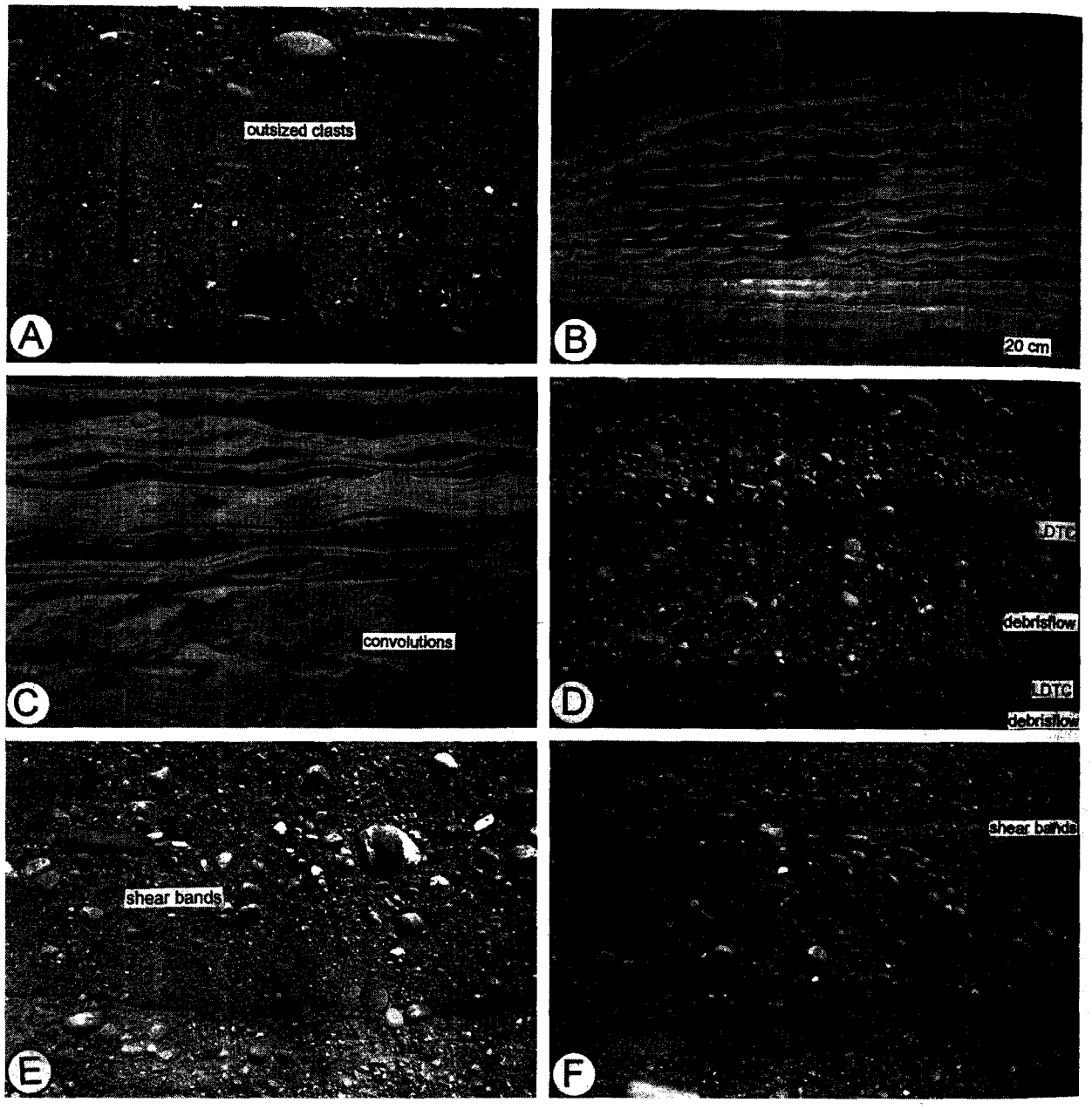

Fig. 3. Close-up details of the delta foreset facies: □A. Graded beds T*a* deposited by HDTCs; note the outsized clasts at gravel/sand boundary. □B. Turbidites T*bc*, with climbing-ripple cross-lamination, deposited by sustained LDTCs. □C. Convolutions and highly aggradational cross-lamination in turbidite T*c*. □D. Debrisflow bed and graded turbidite T*a*, separated by sandy turbidites T*b* with vague plane-parallel stratification and scattered pebbles. □E. Debrisflow bed with "coarse-tail" inverse grading, *a*(p)*a*(i) clast fabric and planar shear bands in lower part; the adjacent beds are of same origin. □F. Listric to sigmoidal shear bands in a debrisflow bed. The palaeoflow direction in all cases is to the left. The photographs are parallel to foreset bedding, not showing the depositional inclination. The lens cap in A and D–F is 5 cm and the pencil in C is 11 cm.

of upslope-dipping strata, on the stoss sides of debrisflow mounds in the lower part of the delta slope (Fig. 8, top). The backsets are typically less than 1 m in thickness and consist of coarse to very coarse sand, occasionally including contemporaneous debrisfall gravel entrapped on the stoss incline (Fig. 11A). The backset in a few cases is at least 4–5 m thick, comprising a well-sorted, fine pebble/granule gravel and very coarse sand (Fig. 12B). The fine gravel shows multiple traction-carpet layers (Lowe 1982), 2–4 cm thick, whereas the sand consists of planar parallel strata, mainly 0.4–0.7 cm thick. The origin of the backsets is

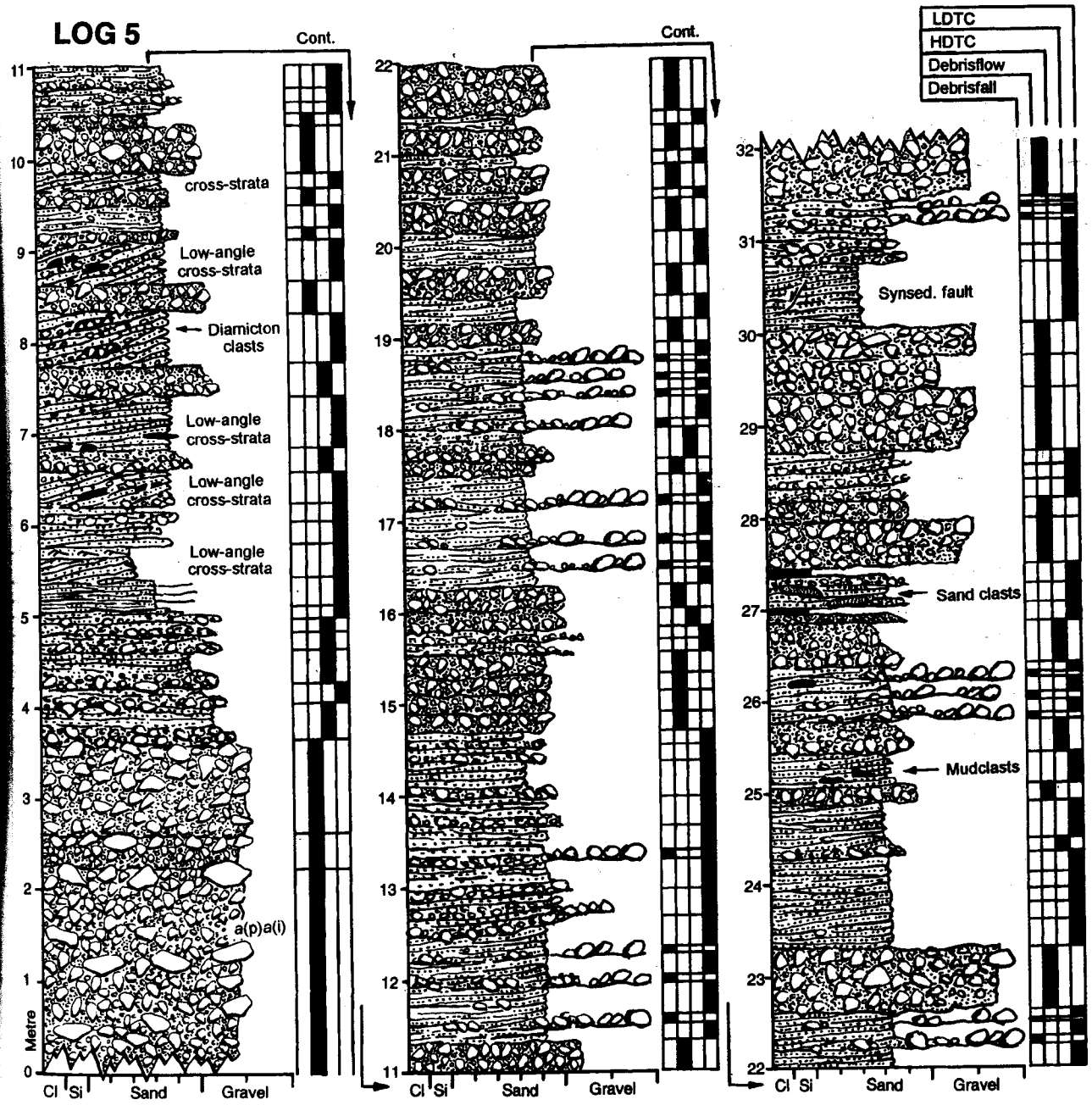

Fig. 4. Sedimentological log 5 (see location in Fig. 2B, C) showing an upper portion of the delta foreset with a genetic interpretation of the component facies. Bed inclination disregarded.

attributed to the hydraulic jump caused by the stoss-side relief of the morphological obstacle (Nemec 1990).

Several isolated sets of low-angle cross-strata downlapping the delta slope are observed in a dip-parallel section of the foreset's middle part (see Fig. 4, left-hand part). The cross-sets are 20–60 cm thick, consist of pebbly coarse sand and are separated by gravelly debrisflow beds of comparable thickness. Each set wedges out upslope and the tangential cross-strata flatten as they downlap the slope, eventually turning into regular foreset stratification. These sand units, apparently turbidites T*b*, are thought to represent small microdelta-type bars (Jopling 1965) formed by sustained LDTCs in the flow-separation zone in the lee of "frozen" debrisflow snouts.

Debrisflow deposits. – Foreset deposits attributed to debrisflows, or non-turbulent sediment gravity flows,

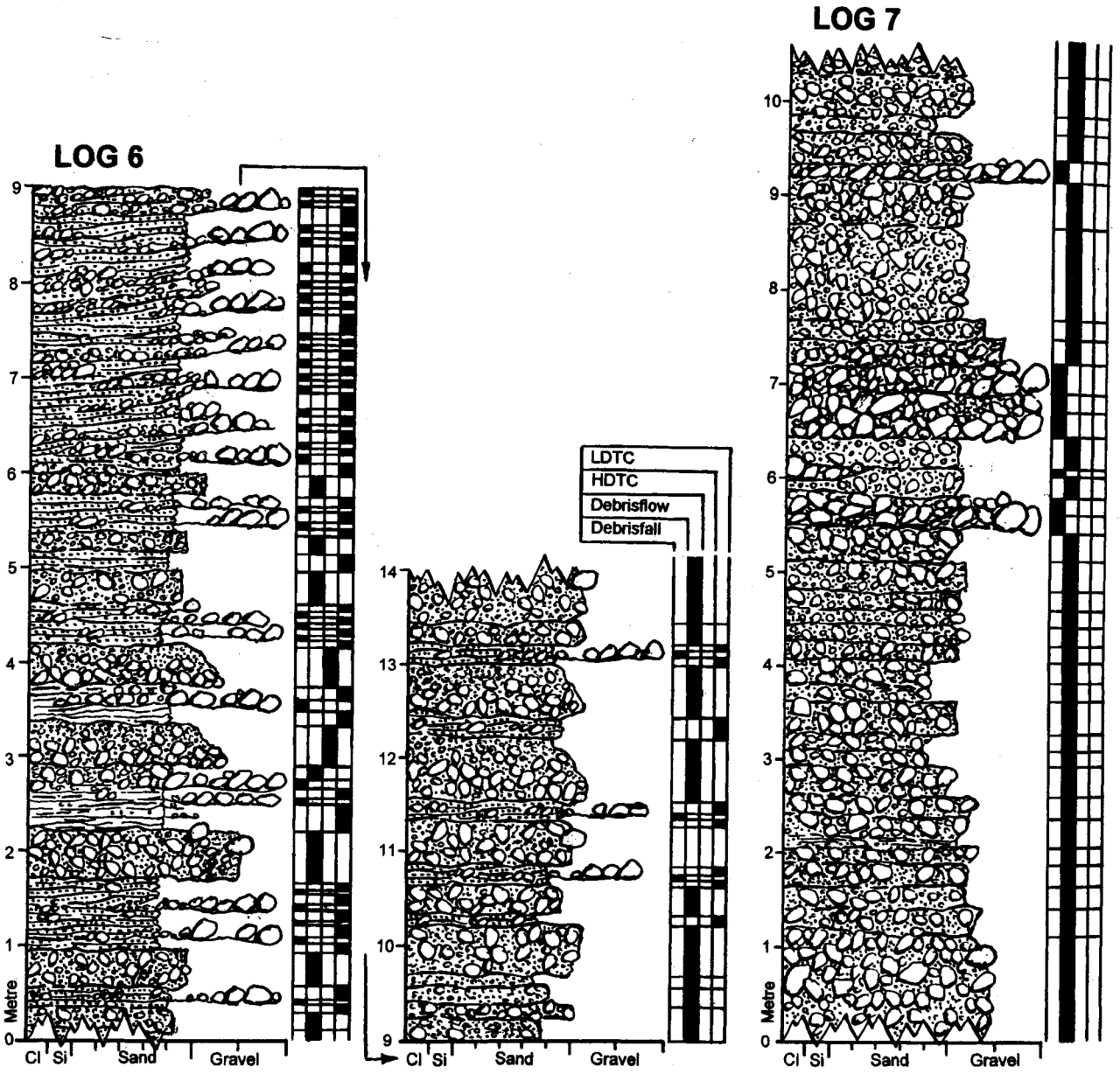

Fig. 5. Sedimentological logs 6 and 7 (see locations in Fig. 2B, C) showing upper distal portions of the delta foreset with a genetic interpretation of the component facies. Bed inclination disregarded.

predominate in the upper part of the delta foreset (see log 4 in Fig, 8; log 7 and upper log 6 in Fig. 5), constitute 40–50 vol.% of its mid-slope part (see upper log 2 in Fig. 6, log 5 in Fig. 4 and lower log 6 in Fig. 5), are subordinate in the lower part (see lower log 2 in Fig. 6 and log 3 in Fig. 8) and nearly absent in the delta-toe turbiditic ramp (see log 1 in Fig. 6). These deposits are beds of pebbly to cobbly sand or sand-supported, pebble- to cobble-sized gravel, mainly 20–130 cm thick, but occasionally as much as 400–500 cm in thickness. A couple of diamictic, mud-rich debrisflow lenses have been found in section 2 (Fig. 2B), where they were likely derived from the fjord-side wall, or melted out from floating icebergs drifted upfjord from another tidewater ice-front. The vast majority of beds have a sand matrix nearly devoid of mud, and these debrisflows were probably cohesionless (Nemec & Steel 1984), controlled chiefly by the sediment's frictional strength, which would explain their low mobility and preferential deposition on the delta's upper to middle slope.

In dip-parallel sections, the debrisflow beds are

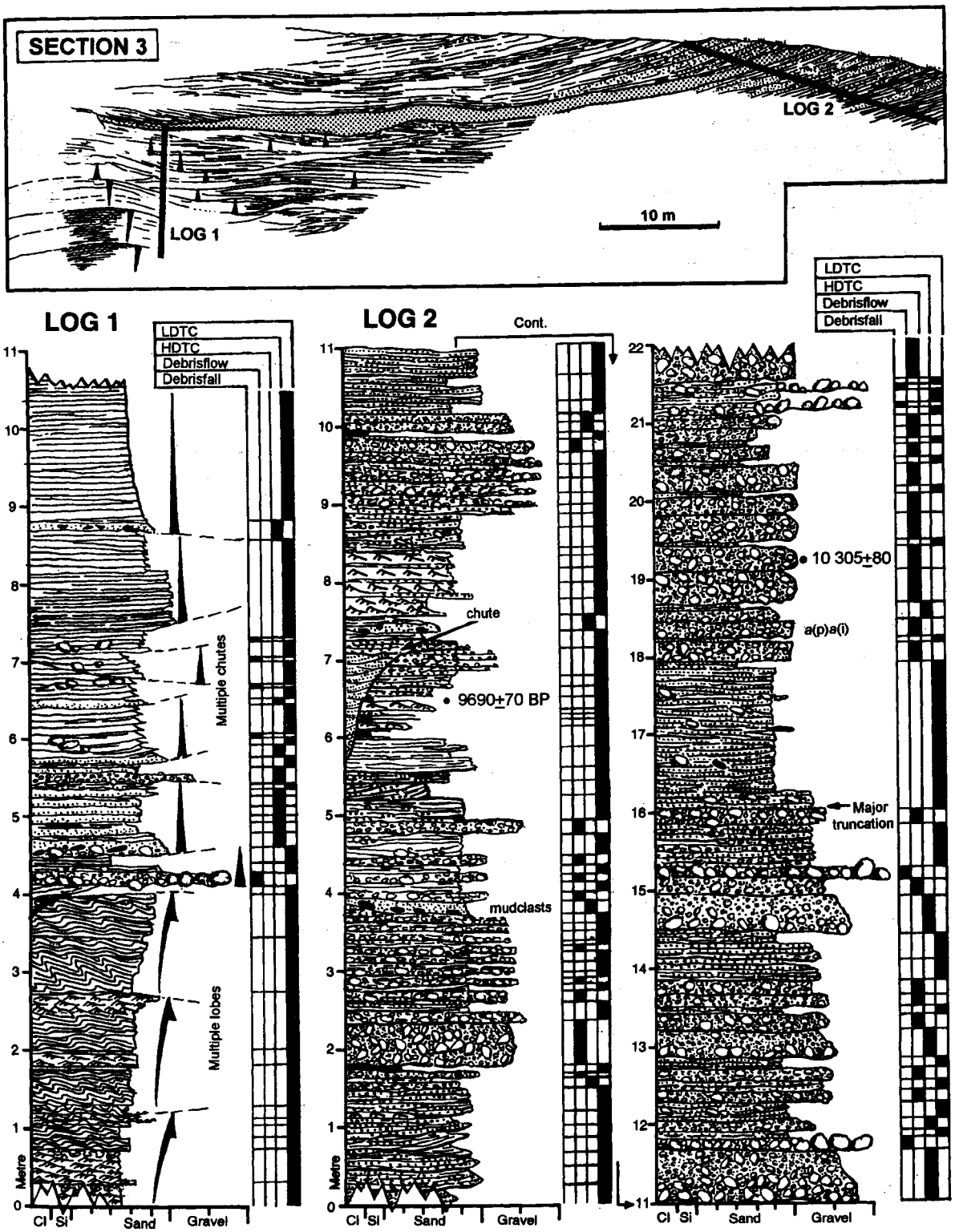

Fig. 6. Sketch of a portion of outcrop section 3 (see location in Fig. 2B) and the corresponding sedimentological logs showing parts of the delta foreset's toe (log 1) and lower slope (log 2), with a genetic interpretation of the component facies. Note the multiple sand lobes overlain by multiple chutes at the delta toe. The palaeotransport direction in the outcrop is to the left, slightly out of the picture. Bed inclination is ignored by the logs.

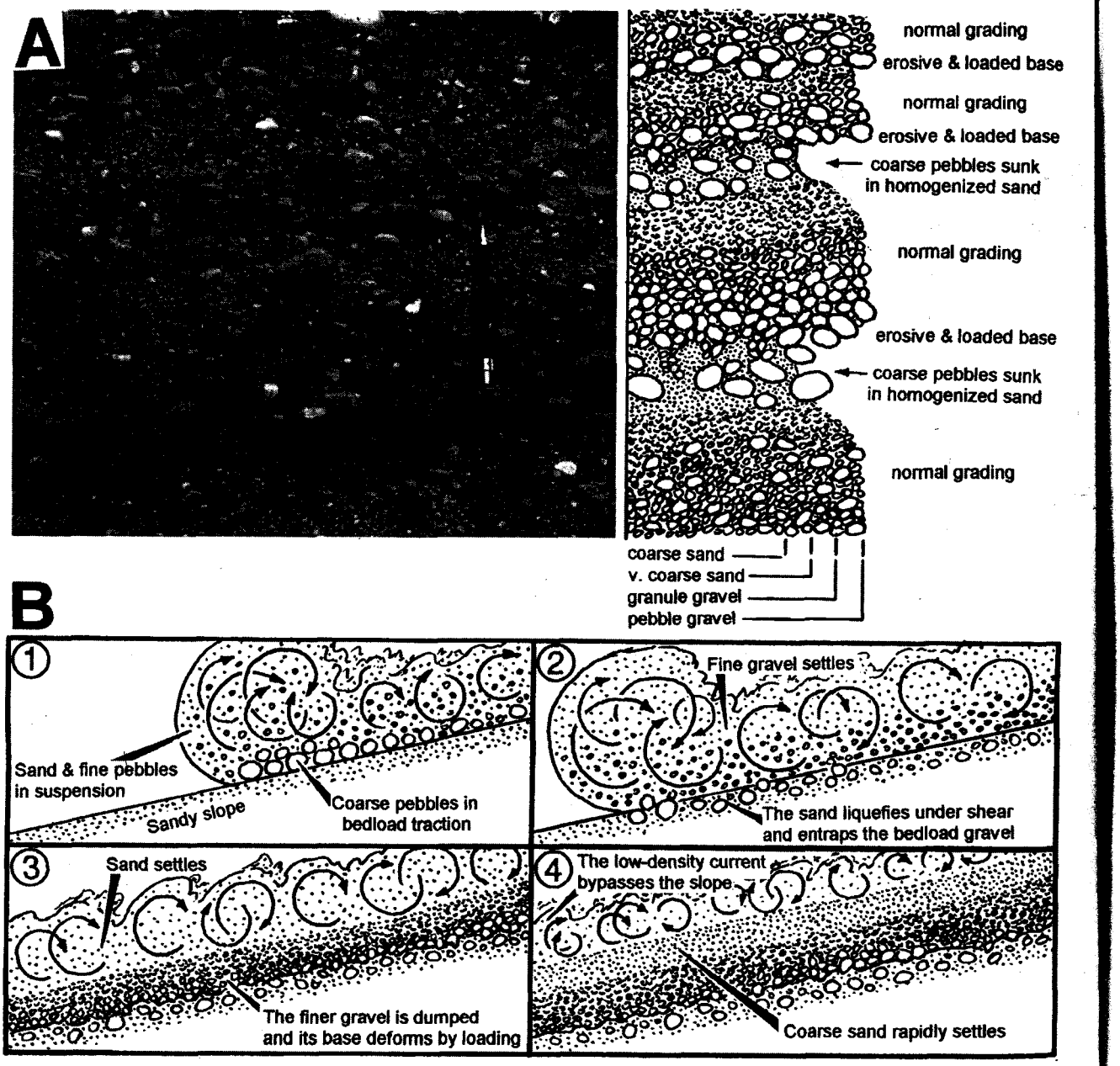

Fig. 7. □A. Foreset beds deposited by HDTCs, showing unusual couplets of a graded fine-pebble to granule gravel overlain by a homogeneous sand with floating large pebbles and deformed top; detail from the upper part of log 3. □B. Interpretation of the couplet origin: (1) a gravel-laden turbidity current arrives on a sandy delta slope; (2) the current's basal shear stress liquefies the sandy substratum, which consequently entraps the coarse bedload gravel; (3) the decrease of the current's energy by the bottom shear causes rapid settling of the fine gravel from suspension; and (4) the depletion of the current's mass causes further deceleration and a rapid dumping of the coarser sand, while the finer load is carried by the remaining low-density current to the delta toe. Note that the pebbly sand layer in *A* would thus be the upper part of a turbidite into which the coarse bedload clasts of the subsequent current have sunk.

extensive and fairly tabular, although many pinch out abruptly downslope and/or are thinning upslope. Strike-parallel sections show lenticular bed geometries, with little or no basal scour. The beds abound in floating outsized clasts and are most often ungraded (Fig. 3D) or "coarse-tail" inversely graded (Fig. 3E), particularly in the basal parts. This type of grading is attributed to the loss of the largest (heaviest) clasts from the lower, faster-shearing and rheologically weakest part of a debrisflow (Naylor 1980). The scarcity of normal grading at the bed tops suggests relatively slow, low-mobility debrisflows, with negligible shear and no

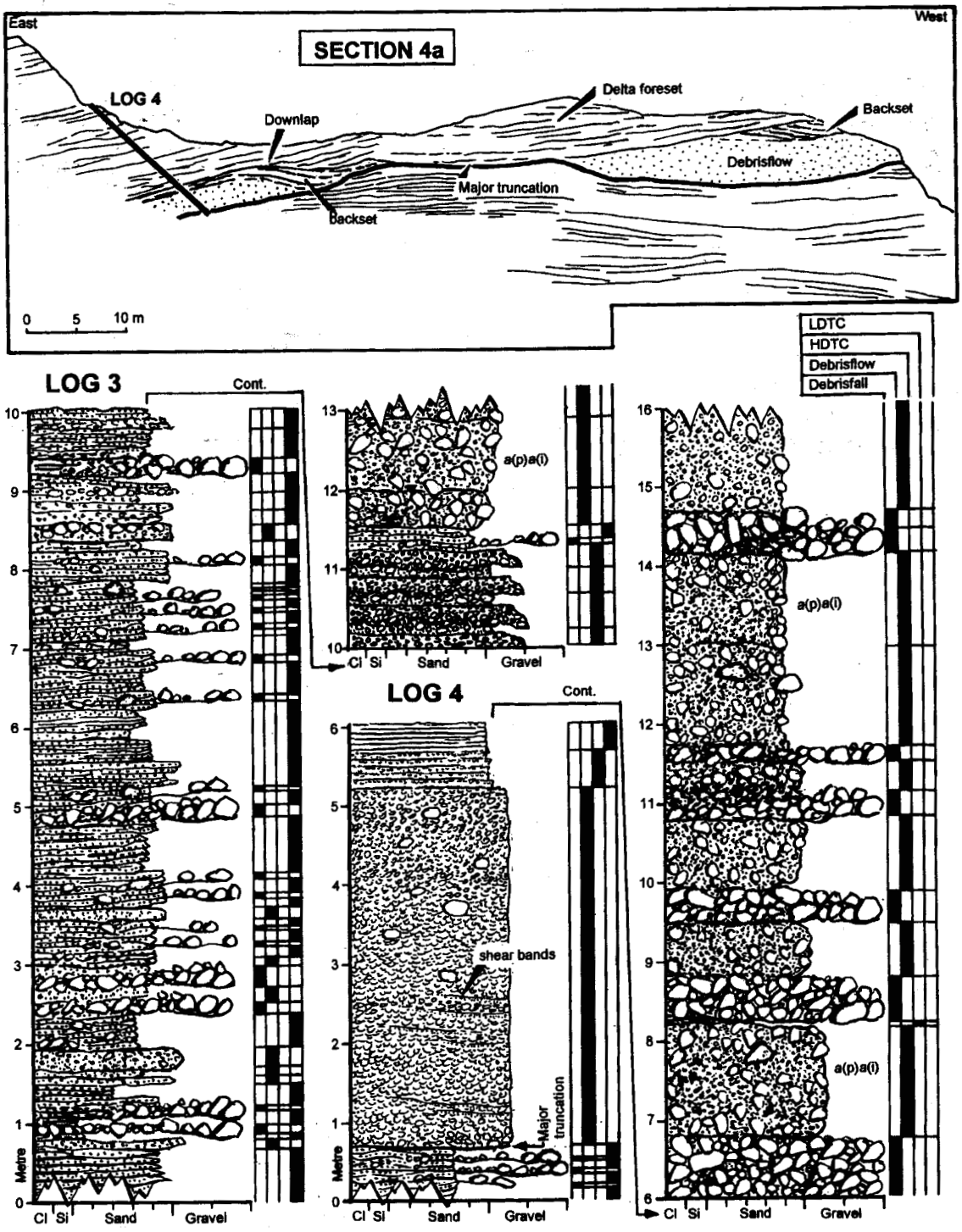

Fig. 8. Sketch of outcrop section 4a (see location in Fig. 2B) and the corresponding sedimentological logs showing portions of the delta foreset's middle part (log 4) and lower part (log 3), with a genetic interpretation of the component facies. Log 3 is a downdip equivalent of log 4, located a few tens of metres to the left in the outcrop section; bedding inclination disregarded. The direction of delta progradation in the outcrop sketch is towards the viewer, obliquely (*c.* 30°) to the left. Note the extensive erosional surface overlain by thick debrisflow deposits and associated turbiditic backsets, attributed to a major collapse of the delta slope.

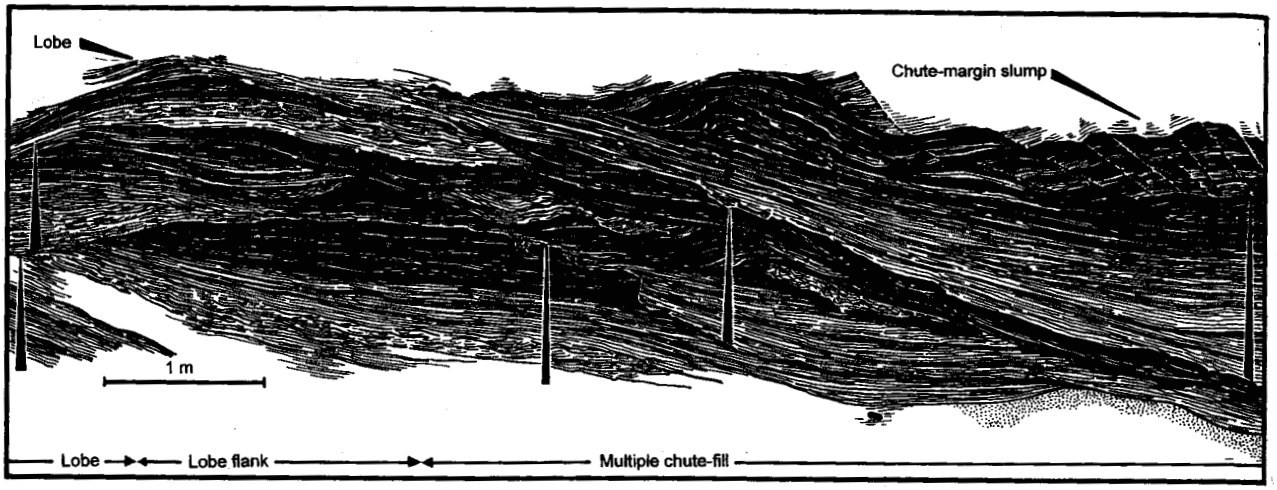

Fig. 9. Multiple chutes overlying delta-toe sand lobes in outcrop section 3 (Fig. 2B, C; see also log 1 in Fig. 6). Sketch made as an overlay drawing from a photomosaic. The palaeotransport direction is out of the picture, obliquely to the left.

turbulent churning at the upper interface (cf. Hampton 1972). Many beds show an *a*(p) or *a*(p)*a*(i) clast fabric, attributed to laminar shear. Some beds show upslope-dipping internal shears, listric or sigmoidal in shape, marked by pebble stringers or sandy bands nearly devoid of gravel (Figs. 3F, 12B). These features are thought to be syndepositional thrusts, self-inflicted by the debrisflow body in response to an abrupt frontal braking (Nemec 1990).

The debrisflows are thought to have been spawned by the gravitational failures of the delta brink zone and uppermost slope. The sporadic mud-rich debrisflows were probably derived from the fjord-side slope or some inactive, slack-water parts of the collapsing delta front. The thickest debrisflow bodies, forming large mounds smoothed by turbiditic backsets (see previous facies), overlie extensive erosional surfaces and apparently represent major collapses of the delta slope (see outcrop section 4a in Figs. 8 and 12A). These debrisflow units consist of coarse sand rich in fine gravel and show abundant shear bands, which may explain their bulged geometry and unusually high thickness. When the front

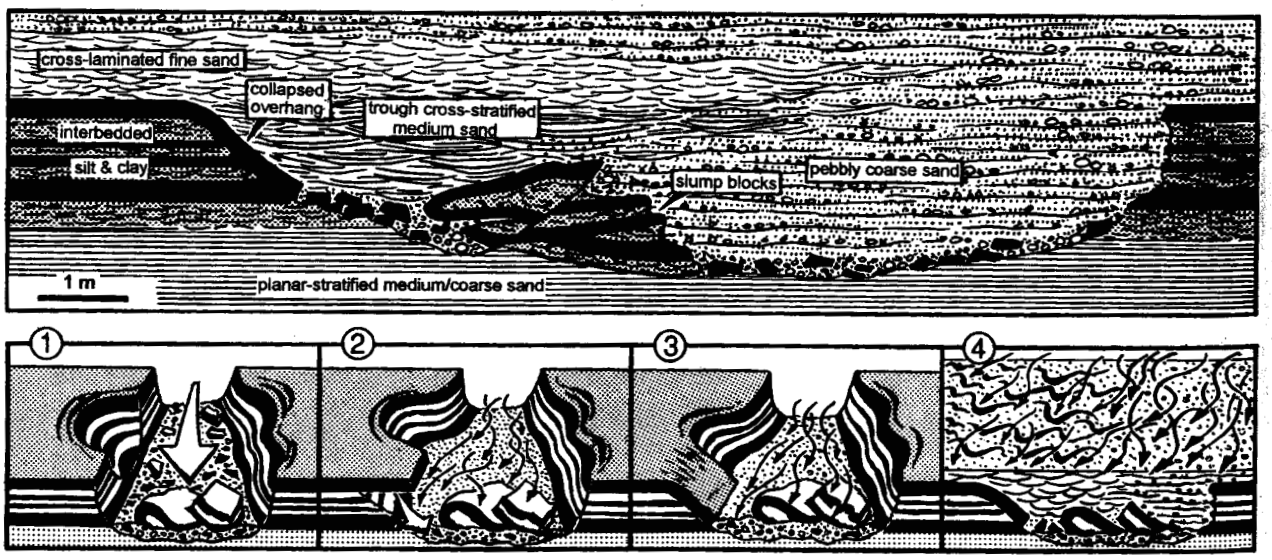

Fig. 10. Outcrop sketch of a chute, or slope-collapse gully, in the lower middle part of the delta foreset (palaeotransport direction towards the viewer, obliquely to the left) with a corresponding cartoon interpreting the chute-fill processes. The through cross-stratification in the chute-fill is attributed to the formation of 3-D dunes caused by turbidity current confinement, but may alternatively be a series of scour-and-fill features comprised of turbidites T*b*; either scenario implies a sustained, low-density turbidity current. Detail from outcrop section 2 (Fig. 2B, C).

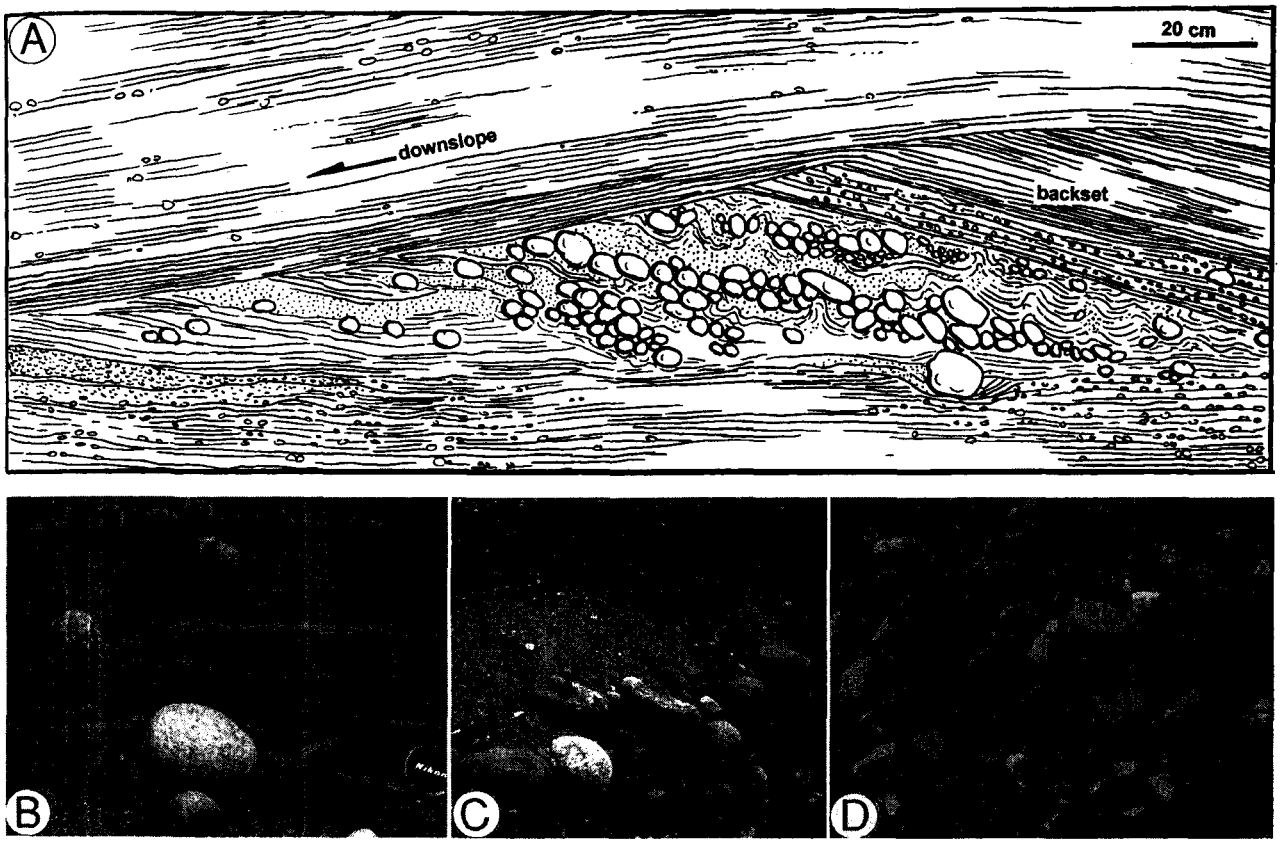

Fig. 11. □A. Backset in the lower part of the delta foreset, showing abundant debrisfall gravel entrapped on the stoss side (see also Fig. 13B, lower part). □B. Scattered debrisfall clasts in the toe part of the delta foreset; the downslope direction is to the left and the lens cap is 5 cm. □C. A cluster of debrisfall clasts in the lower part of the delta foreset, showing *a*(t) *b*(i) fabric; the downslope direction is obliquely towards the viewer and the pencil is 11 cm. □D. An accumulation of debrisfall gravel (portion of a lenticular gravel bed) in the lower part of the delta foreset; the downslope direction is obliquely to the left and the lens cap is 5 cm.

of a moving debrisflow abruptly brakes, the "freezing" flow body often rapidly thickens by discrete shear in an attempt to overpass the obstacle (Nemec *et al.* 1988; Nemec 1990).

Debrisfall deposits. – Deposits attributed to debrisfall processes (*sensu* Nemec 1990) are of minor volumetric importance. They occur at all levels of the delta foreset, but are most abundant in its lower part (see log 3 in Fig. 8). These deposits range from scattered, isolated or clustered cobbles (Fig. 11A–C), commonly associated with turbidites T*b*, to distinct lenticular beds of cobble to coarse pebble gravel, 20–60 cm thick (Fig. 11D). The gravel lenses often show a cobbly "head" passing upslope into a pebbly "tail", and their texture tends to be openwork, at least in the basal head part. The substratum, if a stratified sand, commonly shows some deformation indicative of clast impact and/or loading, with the cobbles bending or denting the underlying strata, or there is evidence of the clast having been undermined by the vortices of a coeval turbidity current (Fig. 11B).

The gravel lenses are invariably clast-supported (Fig. 11D), but their openwork texture is better preserved where the overlying bed is a debrisflow deposit, rather than a turbidite (e.g., in log 7 in Fig. 5). Similarly, the "rolling" fabric of *a*(t) or *a*(t)*b*(i) type, which often characterizes rockfall/debrisfall deposits (Blikra & Nemec 1998), is poorly developed in the gravel lenses and seldom recognizable where the scattered gravel is associated with turbidites (Fig. 11). The falling clasts have probably collided with one another and adjusted their resting positions to the static slope debris. Furthermore, the turbidity currents probably tended to reorient the scattered cobbles, which must have acted as obstacles to currents whose transport competence was often barely enough to carry granule or fine-pebble gravel. This suggestion is supported by the common evidence of stoss-side "horseshoe" scours around isolated cobbles and large pebbles (Fig. 11B, bottom).

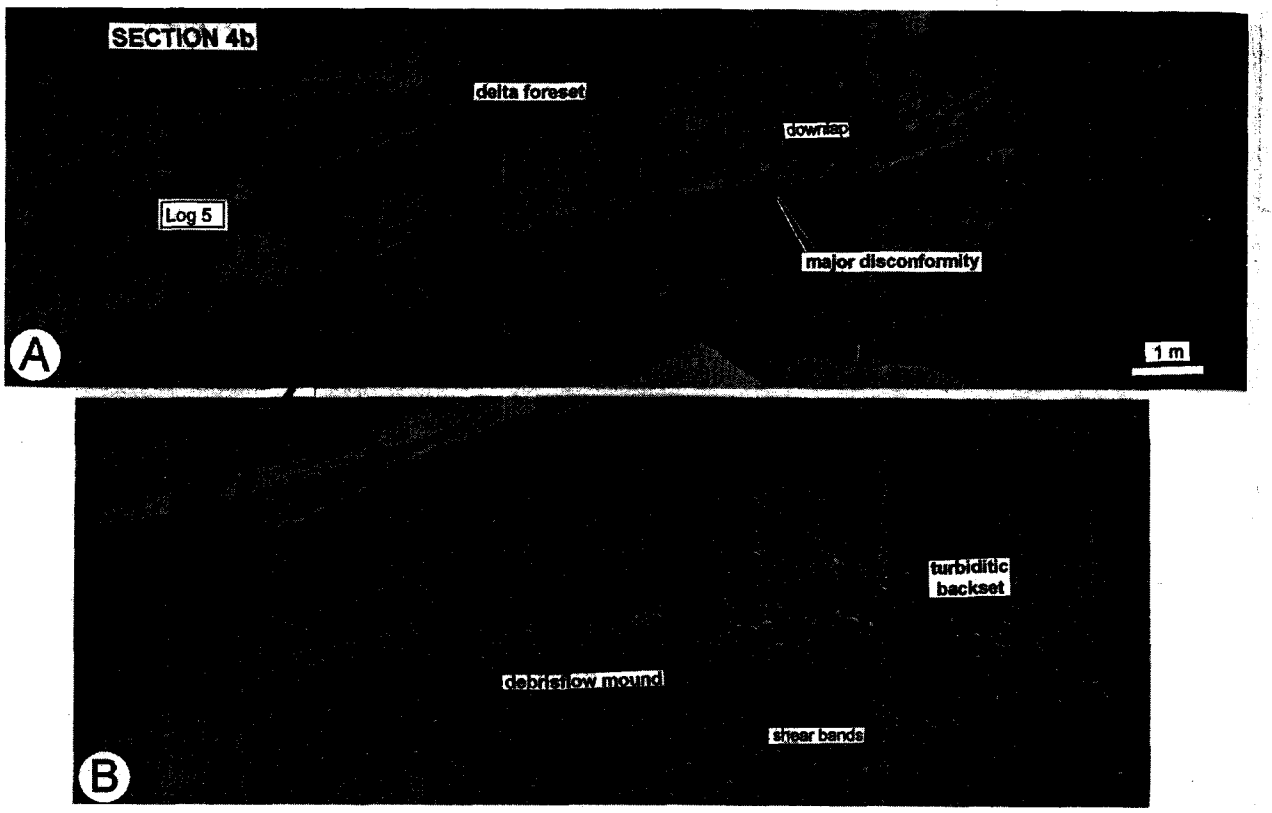

Fig. 12. □A. Portion of the delta foreset in outcrop section 4b (Fig. 2B), showing an extensive disconformity downlapped by deposits of reactivated delta slope. □B. Close-up detail of the outcrop's lower part, showing a thick debrisflow mound overlain by large turbiditic backset; the textural continuity between the two units suggests that the debrisflow was directly followed by the turbidity current and they probably resulted from the same retrogressive slope failure. The debrisflow deposit overlies a major truncation surface in the delta foreset (see also Fig. 8, top). The downslope direction is to the left.

The debrisfall gravel is thought to have been derived from the delta brink zone, whose collapses probably involved the outlets of gravel-bed distributary channels. The slumping processes, producing debrisflows and turbidity currents, most likely created steep local headscarps, mainly short-lived, from which the coarsest gravel tumbled freely downslope as isolated clasts or loose clast assemblages.

Other features. – The multiple delta-toe sand lobes overlain by multiple palaeochutes (log 1 in Fig. 6) suggest that the delta was advancing by the alternating episodes of slope-base aggradation and progradation. The toe of the delta slope aggraded in response to the slope steepening, causing intense sediment sloughing by means of chutes and occasional large-scale failures. For example, the delta foreset in sections 3 and 4 (Fig. 2B) shows at least two internal truncation surfaces that are broadly listric, extend over the entire foreset height and are lined with the thick debrisflow mounds smoothed by turbiditic backsets (e.g., see Fig. 8, top). These internal disconformities, downlapped by reactivated foreset (Figs. 12A, 13A), indicate occasional major collapses of the delta slope. It is likely that the delta has experienced several such failures during its northward progradation. Shell fragments from a chute-fill 6 m below the first recognizable truncation surface and from a debrisflow bed 3 m above it (see log 2 in Fig. 6) have yielded radiocarbon ages of 9690 ± 70 and $10\,305 \pm 80$ BP, respectively, but the odd young date from apparently older deposits is considered to be unreliable (see Table 1 and later discussion).

The load of the downlapping, reactivated gravelly foreset is thought to have caused slope creep that resulted in a "pressure ridge" recognizable in section 3 (Fig. 13A). The deformed portion of deposits is a unit of planar parallel-stratified, very coarse to coarse turbiditic sand, *c.* 1 m thick, that shows a large open fold accompanied by smaller asymmetrical folds (Fig. 13B), indicating marked tangential deformation. It is likely that the underlying backset mound of coarse sandy turbidites T*(a)b* with cobbly debrisfall gravel (Figs. 13B, 11A) has acted as an obstacle to creep and localized the compressional deformation.

In the upvalley section 1 (Fig. 2A), the foreset deposits exposed at an altitude of *c.* 20 m show clear

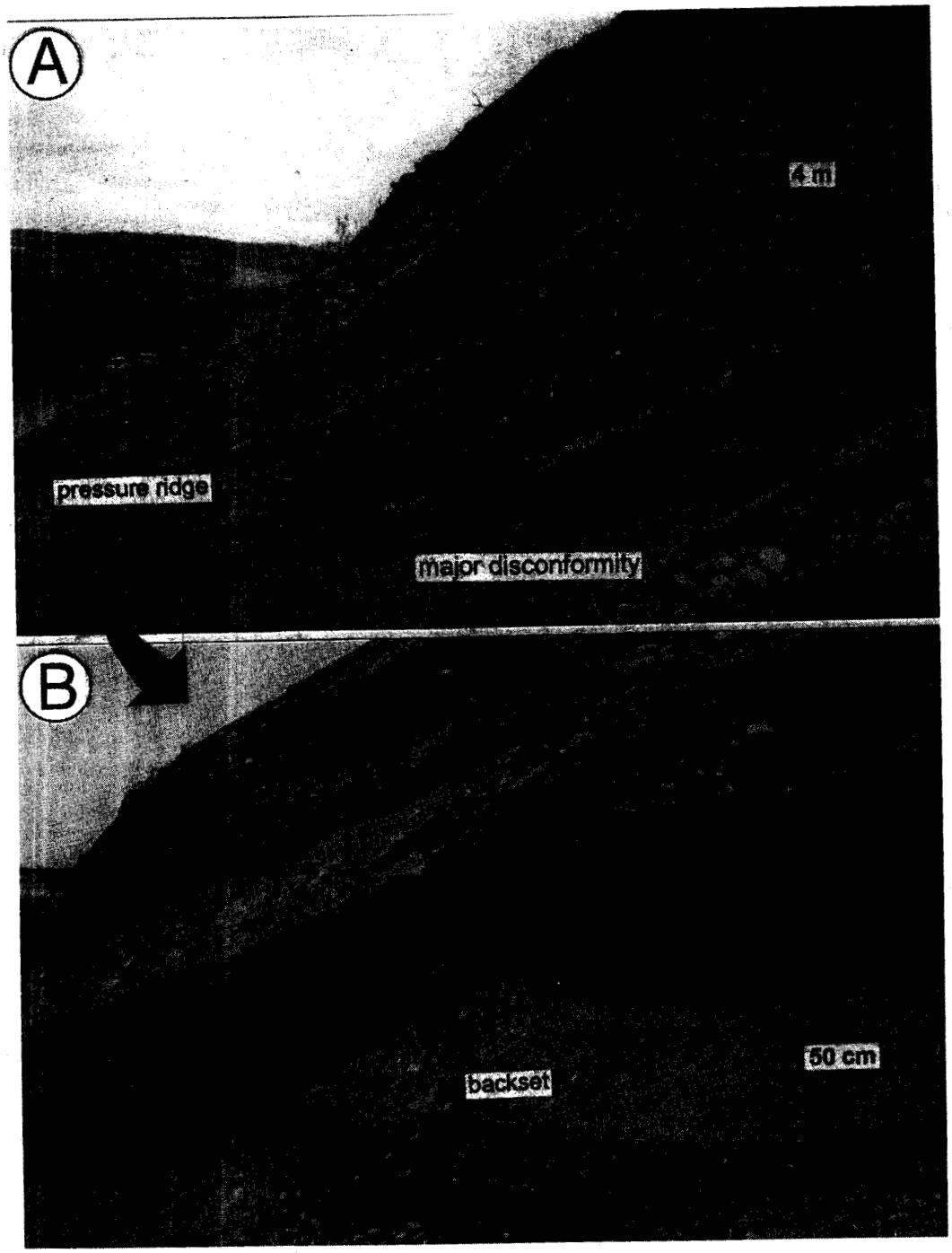

Fig. 13. □A. Portion of outcrop section 2 (Fig. 2B), showing an extensive disconformity downlapped by deposits of reactivated delta slope; note the "pressure ridge" at the downslope tip of the wedge-shaped package of the downlapping, gravelly foreset strata. □B. Close-up view of the "pressure ridge" and the underlying backset; note the small asymmetrical folds within the open-fold ridge. The backset overlies a major truncation surface in the delta foreset and is covered with a thick turbidite T*b*, attributed to sustained LDTC.

evidence of glacitectonic deformation, in the form of southward-dipping listric thrusts and associated, north-vergent recumbent folds. This locality corresponds with a south-sloping escarpment, 60–70 m in relief, that marks the upvalley limit of the depositional system and is interpreted to be the ice-contact surface (Fig. 2B). No glacitectonic deformation is recognizable in the delta's outcrop sections further to the north.

Table 1. Radiocarbon dates of marine fossils from the Kregnes delta. The TUA samples were dated by the AMS technique and the other two samples (courtesy of T. Moseid) by conventional method. The ages are in noncalibrated radiocarbon years, but have been corrected for the isotopic effect of basinal water (440 years).

Sample	Laboratory ref. no.	Material	Age (yrs BP)	Host facies	Outcrop section
1	TUA-742	Unspecified shell fragments	9690 (±70)	Delta foreset	3
2	TUA-1036	Unspecified shell fragments	10 305 (±80)	Delta foreset	3
3	TUA-966	Unspecified shell fragments	10 370 (±75)	Palaeobeach	2
4	T-11071	*Mya truncata* shells	10 155 (±130)	Palaeobeach	2
5	T-11072	*Balanus* sp.	10 520 (±140)	Palaeobeach	2

Topset facies

Relicts of the delta's horizontally bedded topset are preserved, as forested terraces, in outcrop sections 2 and 5 (Fig. 2B, C). The deposits represent braided-river alluvium, but include a delta-front palaeobeach and associated, fjord-side nearshore deposits.

Fluvial deposits. – In the northern part of the delta (section 5), the topset succession is 2.5–3 m thick and shows a gravel lag overlain by cross-stratified sand (Fig. 14A). The lag has a thickness of 20–30 cm and consists of unstratified pebble gravel. The overlying sand is very coarse to medium grained and planar cross-stratified, with finer-grained, ripple cross-laminated interbeds in the upper part. The cross-strata coset is unidirectional, includes both tabular and wedge-shaped sets of tangential strata, and abounds in tangential internal scours (reactivation surfaces *sensu* Collinson 1970). The cross-lamination represents mainly climbing ripples with erosive stoss sides. The succession shows an overall upward fining (see inset log in Fig. 14A). The underlying foreset is coarser, more gravelly, than the topset. The contact of the foreset beds with the topset base is angular, as in the "fluvial-dominated" Gilbert-type deltas of Colella (1988, fig. 18).

The succession is interpreted to be a fluvial channel-fill. The erosive gravel lag is apparently a channel-floor deposit, whereas the overlying coset of planar cross-strata represents a compound bar formed by the vertical stacking of 2-D and 3-D dunes, with numerous phases of erosion and reactivation (Collinson 1970). The upward fining and the predominance of climbing ripples at the top suggest channel abandonment phase. The palaeochannel depth would then correspond roughly to the succession's thickness of 2.5–3 m.

In the southern part of the delta (section 2), the topset succession is 2–3 m thick and consists of sandy coarse-pebble gravel, whereas the underlying foreset is finer grained, composed of alternating coarse sand and fine-pebble gravel. The topset deposits show horizontal stratification and planar cross-stratification, with cross-sets thicknesses of 0.5–1 m, and are locally underlain by a cobbly basal lag, 20–25 cm thick. The palaeotransport direction is consistently towards the north. The contact of the foreset beds with the erosive topset base is angular, but the upper part of the foreset shows local internal truncations (short reactivation surfaces) that are convex upwards and overlain by stratified gravel wedges (Fig. 14B). These isolated wedges have maximum thicknesses of 0.5–1.5 m, pinch out in the downdip direction, at a depth of 5–6 m below the topset, and their tangential contact with the topset is as in Colella's (1988, fig. 18) "wave-influenced" Gilbert-type deltas.

The sedimentary features of the topset indicate a bedload river dominated by gravel and sand braid-bars. The fjord's wave base was apparently quite shallow, not exceeding the depth of the fluvial channel incision. The convex-upward reactivation surfaces and associated gravel wedges in the uppermost foreset are attributed to an episodic reworking of the delta front by storm waves, which would imply the storm wave base occasionally reaching a depth of 6 m, probably due to strong, fjord-parallel southward winds (maximum wave-fetch conditions).

It is common in Gilbert-type deltas that the grain-size characteristics of the fluvial topset at a particular locality do not match strictly those of the underlying foreset, simply because the branching distributary channels tend to shift, vary in space and time, and their infilling is obviously not coeval with the deposition of the foreset over which they have extended seawards.

Marine deposits. – Near the palaeofjord's bedrock sidewall in section 2, the fluvial deposits are overlain by a unit of sandy gravel, *c.* 1 m thick (Fig. 14C), whose subhorizontal stratification and textural segregation of gravel into extensive layers suggest deposition as a delta-front beach. The altitude of this horizontal unit corresponds to the local marine limit. The size sorting of gravel is moderate and shape segregation is poor, compared to well-developed reflective beaches (Massari & Parea 1988; Postma & Nemec 1990), and also the roundness of clasts is highly varied (Fig. 14D), generally poorer than in the underlying fluvial facies. The common occurrence of disintegrated full-form clasts, split *in situ* along the cleavage planes and fractures, indicates significant gravel shattering by frost action (Blikra & Longva 1995), which has certainly contributed to the apparent angularity of the debris. The low textural maturity of the beach gravel can further be

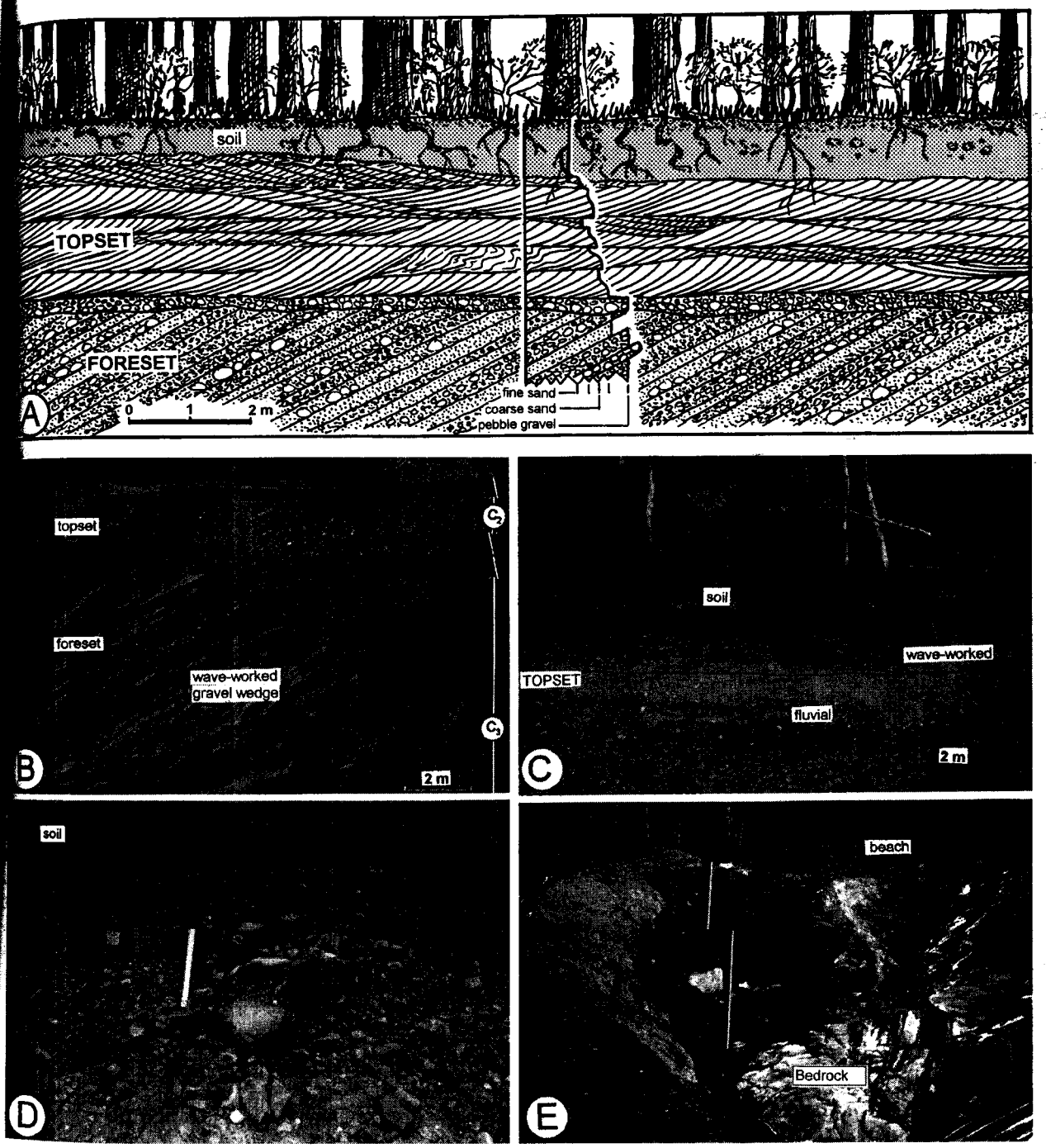

Fig. 14. Details of the delta topset: □A. Outcrop sketch of the fluvial topset in section 5 (Fig. 2B, C), with an inset log. □B. The topset/foreset contact in outcrop section 2 (Fig. 2B, C), showing an isolated convex-upward truncation and associated gravel wedge in the uppermost part of the foreset; labels C_2 and C_3 refer to the allostratigraphic units in Fig. 15. □C. Gravelly fluvial topset overlain by thin palaeobeach in outcrop 2; note the large boulder block resting on the forested surface of the palaeobeach terrace. □D. Close-up view of a coarse palaeobeach gravel where frost-shattering has been recognized. □E. Fjord-side shoreline deposits adjoining the delta topset, preserved in a bedrock niche and exposed by the delta foreset excavation in gravel-pit section 2; note the coarsening-upward units comprised of mud and sand with scattered coarse gravel, overlain by gravelly palaeobeach, and the intercalation with the delta foreset to the left (towards the viewer).

attributed to the rockfall supply of debris from the adjacent bedrock wall, shattered by frost, and the generally low wave fetch of the fjord basin. The side-wall rockfall processes have apparently continued until the modern times, as is indicated by scattered large boulders, up to 10–15 m long, some of which have been buried or half-buried in the palaeobeach and others rest on its vegetated surface (Fig. 14C).

The palaeobeach deposits laterally overlie, and partly interfinger with, the upper part of a fine-grained succession, whose relicts, 1–3 m thick, are preserved as the infill of local niches in the steep bedrock slope (Fig. 14E). This succession consists of a couple of coarsening-upward mud-sand wedges with minor intercalations of coarse gravel. The mud ranges from laminated to massive, shows scattered pebbles and contains marine fauna, including *Balanus* sp. and *Mya truncata*. Likewise, the overlying sand is pebbly, coarsens upwards and varies from faintly stratified to massive, with local deformation features indicative of slumping. These deposits are thought to represent a narrow, slope-hosted shoreface, sandy to muddy, whose progradation involved episodic gravitational collapses and beach failures (debrisfalls), followed by mud deposition and shoreline re-building. The sand beds show an upward-increasing dip angle and a dip direction towards the W/NW, nearly perpendicular to the fluvial palaeocurrent azimuth and the dip direction of the delta foreset, which suggests a fjord-margin shoreline adjacent to the delta front. The thickest, lowest-reaching relict of the fjord-margin succession rests directly on the delta foreset and seems to be interfingered with the latter, which implies deposition contemporaneous with the delta progradation along the fjord side-wall. The other relicts are more isolated, "hanging" in the wall niches. These fjord-side nearshore deposits, now exposed by gravel-pit excavation, were apparently buried by the prograding delta.

The muddy nearshore facies, overlain by a thin wedge of beach-derived sand and covered with a comparably thin gravelly palaeobeach, support the notion of a generally shallow wave base, apparently no deeper than 1.5–2 m. Shell fragments from the lowermost exposed mud unit have yielded a radiocarbon date of 10 370 ± 75 BP, and the faunal remains from two other mud units, sampled by T. Moseid (pers. comm. 1994), have yielded dates of 10 155 ± 130 and 10 520 ± 140 BP (Table 1). The occurence of frost-shattered gravel in the palaeobeach is consistent with the Younger Dryas age of the delta (see Blikra & Longva 1995).

The style of delta progradation

The preceding facies analysis demonstrates that the Kregnes "moraine" is a proglacial Gilbert-type delta, deposited in the Gauldalen palaeofjord in the middle Younger Dryas time. The facies assemblages suggest that the delta has been advancing through alternating episodes of delta-toe aggradation and progradation, related to the increases and decreases of the delta-slope gradient.

The delta's avalanching slope was accumulating deposits of high-density turbidity currents, debrisflows and debrisfalls, whereas the low-density turbidity currents were mainly bypassing the slope and depositing their sandy and muddy load in the bottomset and prodelta zone, respectively. The turbidity currents were mainly of sustained type, but dropping their gravel and coarse sand load on the delta slope in a surge-like fashion. Ubiquitous mud was probably carried to the prodelta zone by the delta's hypopycnal suspension plume (Nemec 1995), causing high-rate aggradation of the fjord floor.

The angle of the delta slope was increasing due to the sediment accumulation, leading to intense sloughing by chutes or slope-collapse gullies (Prior *et al.* 1981; Nemec 1990; Prior & Bornhold 1990), while the sharpened slope break at the delta toe led to hydraulic-jump conditions. As a result, the intensified low-density turbidity currents were forced to deposit most of their load directly at the delta toe, forming multiple aggradational sand lobes. The slope sloughing and toe aggradation rendered the delta slope more gentle, increased its sediment accumulation capacity and led to bulk progradation, with the turbidity currents again able to spread freely their load over the slope-base and prodelta zone. The whole "feedback" cycle would then repeat itself, with the slope steepening occasionally leading to large-scale failures followed by foreset reactivation. The high rate of mud accumulation in the fjord made the prograding delta's toe climb against the quickly aggrading basin floor. The relatively thin topset with horizontal erosive base implies stable sea level. The radiometrically constrained ice-front movement curves from the last deglaciation of Scandinavian fjords (e.g., Andersen *et al.* 1995b) indicate that the episodes of "moraine" formation were relatively brief, with time-spans beyond the resolution of radiocarbon dating, but probably on the order of decades to a century. Therefore, it is unlikely that the formation of an ice-front mid-fjord system such as the Kregnes delta may have taken more than a hundred years. The delta toe has climbed by 50 m during the delta-front progradation over a distance of 1.5 km. Assuming a time-span of less than hundred years, this would imply a basin-floor aggradation rate in excess of 50 cm/yr. The rate of the delta-front progradation was probably non-linear, increasing due to the basin's decreasing accomodation space (shallowing), but the mean rate could be higher than of 15 m/yr.

Allostratigraphic facies architecture

The facies anatomy of a depositional system, although

reflecting well the spatial pattern of sedimentary processes, may not necessarily reflect fully the system's stratigraphic development, because the coeval processes may widely vary and a whole range of diverse facies may form along the system's "time surfaces", whereas similar facies may correspond to different developmental stages. In short, the sedimentary facies architecture has to be considered in terms of a dynamic time-stratigraphic framework appropriate for a particular type of sedimentary system. In this section, we discuss the development history of the Kregnes delta in terms of the conceptual allostratigraphic model developed by Lønne (1995), which has proven to be a useful tool for the analysis and comparative studies of ice-front sedimentary systems (Lønne 1997b; Lønne & Syvitski 1997).

The aim of allostratigraphy is to recognize the main changes in a depositional palaeosystem, both autogenic and allogenic, based on the principal facies packages and their bounding surfaces (Walker 1992). The Lønne model distinguishes the following principal allostratigraphic units: the ice-contact deposits formed during the glacier advance (unit A) and stillstand (unit B); the ice-front deltaic deposits (unit C); the ice-distal deposits formed during the glacier retreat (unit D); and the deposits formed during the glacio-isostatic uplift of the system (unit E). Each unit is further divided laterally into coeval subunits according to the morphological position in the system, using the following subscripts: 1 = the ice-proximal side; 2 = the top; 3 = the ice-distal slope; and 4 = the base of the ice-distal slope (e.g., unit C is divided accordingly into subunits C_1, C_2, C_3 and C_4). Suffix *d* denotes glacitectonic deformation. The model thus combines stratigraphic, dynamic and geomorphic aspects, and can serve as a predictive tool for the reconstruction of incompletely exposed ice-front palaeosystems.

The depositional model for the Kregnes delta (Fig. 15) includes five allostratigraphic units, two of which are exposed (units A*d* and C), two are inferred from the palaeosystem's morphology and facies anatomy (units B and E), and one is implied by the physical concept (unit D). The term "apparent ice-contact surface (AICS)" refers to the topographic escarpment on the ice-proximal side of the palaeosystem. This type of escarpment is commonly considered to be the evidence of an ice-front stillstand, although the actual development of this morphological feature may be quite complex, including ice-front movements during the proglacial systems's build-out. There is no outcrop section in the ice-contact part of the Kregnes delta where the "true ice-contact surfaces (TICSs)" (Fig. 15D) could be recognized, but the presence of these features is implied by the system's origin and inferred depositional and deformational history.

Unit A: ice-contact deposits formed during the ice-front advance

Outcrop section 1 (Fig. 2A) shows a turbidite-dominated, northward-dipping foreset deformed by the northward advance of the ice front. This is the stratigraphically lowest exposed part of the depositional palaeosystem. The outcrop is at an altitude of *c.* 20 m, well below the delta-toe level in section 2 to the north. The foreset beds, when projected upwards, meet the AICS, and there is no reason to believe that this foreset has ever had a subaerial deltaic topset. The turbiditic deposits show glacitectonic deformation and are comparable to those described by Lønne (1997a, b) from ice-contact submarine fans. Accordingly, we interpret this low-lying, deformed foreset as a submarine ice-contact fan (*sensu* Lønne 1995) representing the early phase of the system's development. In the Lønne model, this would be a glacitectonized allostratigraphic subunit A_3 (referred to broadly as unit A*d* in Fig. 15A).

No southward or northward equivalent of unit A*d* is exposed in the area, but the published studies of glacitectonized ice-contact fans (e.g., Benn 1996; Lønne 1997b) have demonstrated that this subunit passes downslope into a bottomset wedge of interbedded debrisflow deposits, turbidites T*b* and debrisfall gravel, with sandy turbidites predominant in the distal part. We infer that a similar bottomset, unexposed, forms the distal part of unit A*d* (see subunit A_4 in Fig. 15A). The glacier probably had a calving tidewater front and we would expect ice-rafted debris in this part of unit A*d* (Lønne 1995). The ice-proximal part of unit A*d* (see subunit A_1 in Fig. 15A) would likely consist of till-bearing deposits heavily affected by subglacial deformation and erosion, with a small thickness and limited preservation potential.

Unit A would necessarily be time-transgressive, because its formation is related to an advancing ice front. Our graphical model depicts only the hypothetical surface of the maximum ice-front advance for this phase (see TICS-A in Fig. 15D).

Unit B: ice-contact deposits formed during the ice-front stillstand

The south-sloping escarpment, 60–70 m high, at the upfjord end of the depositional palaeosystem indicates a prolonged halt of the ice front, when the submarine ice-contact fan would inevitably become subject to rapid aggradation (see unit B in Fig. 15B). This unit is unexposed in the present case, but its deposits are likely similar to those of unit A, with the foreset showing evidence of aggradation, possibly multistorey, punctuated by scour and reactivation (Lønne 1995, fig. 4). The ice-front abutting against the aggrading submarine fan would inevitably lead to the cessation of calving process and the grounding of the glacier.

A well-defined TICS is often developed during an

ice-front stillstand (e.g. Lønne & Syvitski 1997, fig. 6), and there is no evidence that the ice front in the present case has ever advanced beyond the position depicted as TICS-B in the model (Fig. 15D). However, this surface is unexposed and the ice front may not have necessarily been fully halted at this stage.

Unit C: deposits of ice-front delta

The large foreset overlain by fluvial topset and reaching the marine limit indicates that the submarine ice-contact fan, comprised of units A and B, has eventually aggraded to the sea level. This development implies the formation of an ice-contact delta (*sensu* Lønne 1995), characterized by a short distributary plain and still directly influenced by the ice front (unit C in Fig. 15B). The ice front thus became effectively separated from the sea, and it is unlikely that unit C contains any ice-rafted debris, unless shed from externally-drifted icebergs.

The ice-contact delta prograded and evolved into a large glaciofluvial delta (*sensu* Lønne 1995), whose distributary plain extended well beyond any direct mechanical influence of the ice front. The deltaic part of the system (unit C in Fig. 15C) is volumetrically most important, including topset (subunit C_2), foreset (subunit C_3) and bottomset deposits (subunit C_4), as well as a hypothetical thin package of ice-contact deposits (subunit C_1), possibly glacitectonized.

Unit D: ice-distal deposits formed during the ice-front retreat

The proglacial depositional system was finally abandoned due to the southward retreat of the ice front, and the resulting "moraine" ridge thus became passive subject to marine processes. Its downfjord and upfjord edges were most likely influenced by wave action and the surficial part probably became conducive to tidal currents (the present-day tidal range of the region's coast is *c.* 1 m). The marine reworking was likely accompanied by slope failures and resedimentation. The upfjord side of the ridge may have initially accumulated some of the retreating glacier's submarine outwash, but would become increasingly dominated by the abundant fine-sediment fallout from the "ponded" suspension plume and could also be influenced by icebergs (Lønne 1995, 1997a, b). The palaeofjord depth suggests a tidewater glacier, which would retreat rapidly by calving. As the glacier retreated, the whole abandoned ridge became a part of the ice-distal domaine.

The products of this early abandonment phase (unit D in Fig. 15D) may have been removed by later erosion and no recognizable relicts are exposed, but we infer that sediment wedges were almost certainly developed on the ridge's upfjord slope (subunit D_1) and downfjord slope (subunit D_3), and at least one tidal channel and possibly an intertidal flat were formed on the top platform (subunit D_2). This suggestion is supported by the adjoining palaeofjord deposits and the present-day morphology of the ridge (see below).

Unit E: deposits formed during the glacio-isostatic uplift

The retreat of the ice front from the Gauldalen fjord and adjacent areas was accompanied by a regional glacio-isostatic uplift, which accelerated the processes of erosion and resedimentation, caused subaerial exposure and resulted in the present-day morphology of the "moraine" ridge. The transition to phase E is normally accompanied by the cessation of direct sediment supply from the glacier and the onset of "normal" marine conditions (Lønne 1995). The deposits of this phase (unit E) would bear the signatures of a falling shoreline and progressive subaerial exposure, but may be difficult to distinguish from those of unit D (Fig. 15D).

The morphology of the Kregnes ridge indicates the presence of wave-cut terraces on both the upvalley and the downvalley slope (Fig. 15D), although the corresponding deposits are vegetated and unexposed. Furthermore, the youngest palaeofjord deposits directly south of the ridge indicate that a tidal channel must have traversed and dissected the ridge's platform, forming a tidal flood delta on the southern side and possibly an ebb delta on the northern side. The palaeofjord fine-grained marine deposits (mud and fine sand) extend to an altitude of 70 m.

The marine environment was gradually replaced by terrestrial conditions, whereby the abandoned tidal channel was probably taken over by river Gaula and the Kregnes ridge has been further dissected and extensively eroded (Fig. 2A). The river valley is 1 km wide in the southernmost part of the ridge, but 2.5 to 1.7 km wide in its remaining part to the north (see fluvial deposits in Fig. 2A), which indicates a wandering river.

Glacier dynamics and palaeoclimatic implications

The Kregnes ice-front system consists of sand and gravel, whose volume is estimated at nearly 900 km^3. An even greater volume of mud was likely spread along the proglacial fjord by the suspension plume of this large proglacial delta (see Syvitski *et al.* 1987; Nemec 1995). The large volume of outwash sediment suggests a temperate glacier with a very high erosional capability. The valley glacier is thought to have had a tidewater terminus during the deposition of allostratigraphic unit A and the lower part of unit B, and turned into a grounded glacier during the deposition of the upper part of unit B and the whole deltaic unit C (Fig. 15).

Modern studies have shown that the temperate

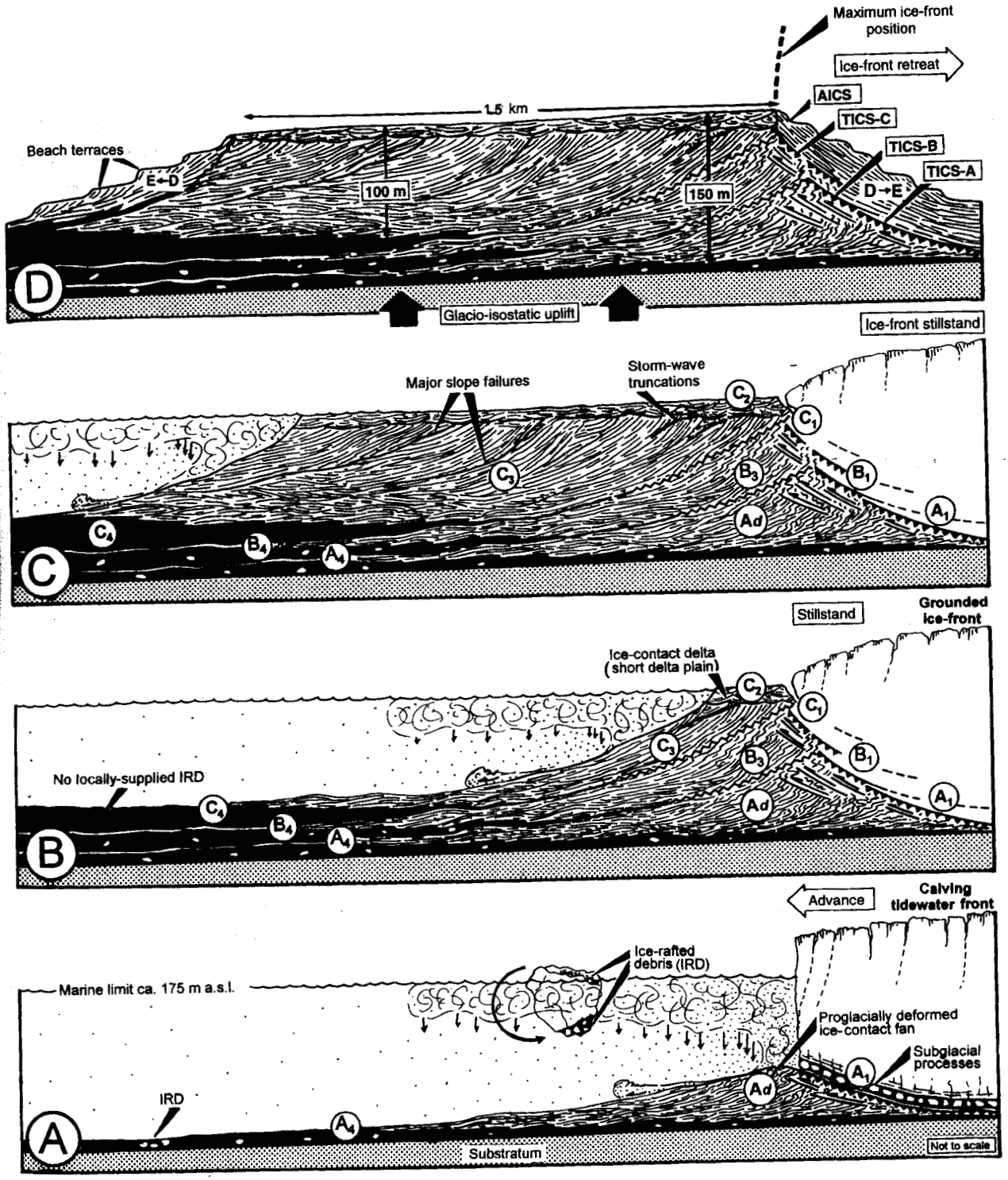

Fig. 15. Allostratigraphic depositional model for the ice-front system at Kregnes in Gauldalen palaeofjord. □A. The advancing glacier comes to a halt on its deformed, ice-contact submarine fan (unit A). □B. The ice-contact fan aggrades during the stillstand (unit B) and reaches the sea surface, turning into an ice-contact delta whose short distributary plain is directly influenced by the ice front (unit C). □C. The ice-contact delta progrades and evolves into a large glaciofluvial delta (main part of unit C). □D. The retreat of the ice front leaves a "moraine" ridge that suffers some marine reworking, emerges due to regional glacio-isostatic uplift and becomes deeply dissected by valley-axis river. The terminology is after Lønne (1995) and the letter symbols with subscripts are as explained in the text; AICS = apparent ice-contact surface; TICS = true ice-contact surface, indicated for units A–C, respectively.

tidewater glaciers in high-relief fjords are controlled by a very delicate physical balance, whereby a glacier may rapidly re-advance without any obvious climatic reason. The causes of such episodic re-advances are not fully understood, but the possible physical factors include: (1) variation in the geometry of the hosting basin and/or the glacier body; (2) a decrease in the size of the ablation area due to increased effective precipitation at higher altitudes; and (3) sediment accumulation at the glacier's grounding line (see review by Powell 1991). Since, a tidewater glacier can shift its front without any regional climatic cause, it has been suggested that the "moraine" ridges, or grounding-line deposits, of such glaciers are unreliable as palaeoclimatic indicators (e.g. Mann 1986). This view, however, is not quite correct.

It has recently been demonstrated (Lønne & Syvitski 1997) that a careful allostratigraphic mapping of the moraine's internal architecture and the recognition of the genetic relationships among its facies assemblages may allow a distinction between "monoepisodic" moraines, such as a simple ice-contact submarine fan related to non-climatic glacial surge (Solheim 1991), and the more compound "polyepisodic" moraines related to phases of climatic deterioration. In short, the moraines of tidewater glaciers may certainly bear some valuable climatic information.

The high calving rate of glaciers in the Alaskan deep coastal waters has led Meier & Post (1987) to conclude that the only way a tidewater glacier can advance in a deep-water basin is by recycling of a frontal morainic shoal (i.e., by eroding and redepositing it in a conveyor-belt fashion), which minimizes calving. Relicts of such "recycled" moraines, in the form of a subglacial deformation layer, have been reported in the literature (Alley *et al.* 1987, Lønne & Syvitski 1997). Meier & Post (1987) have further noted that the cycles of tidewater ice-front advance and retreat are characterized by asymmetrical dynamics: the advance is relatively slow (which can be attributed to the recycling of morainic wedge), followed by stillstand, whereas the retreat is rapid or even catastrophic, as the glacier's decoupling from the moraine leads to intense calving. A sedimentary record of such asymmetrical ice-front fluctuations in deep-water fjords has been discussed by Lønne & Syvitski (1997) on the basis of high-resolution seismic data from Lake Melville, Canada. Their allostratigraphic analysis shows that the advancing tidewater glacier forms a series of wedge-shaped sedimentary units (ice-front advance units A of Lønne, 1995), which are vertically stacked upon one another and overstep each other in a progradational manner. The glacier clearly overrides and erodes the ice-proximal part of one unit while depositing a successive unit upon its distal part. The repetition of this process results in a compound, time-transgressive morainic wedge that both progrades and aggrades. As a consequence of the aggradation, the listric ice-contact surface steepens, the rate of the glacier advance declines and the basal shear stress decreases in a positive feedback fashion. The moraine wedge (or submarine ice-contact fan *sensu* Lønne 1995) at some point becomes sufficiently thick to halt the glacier, which leads to the ice-front stillstand and fan aggradation (allostratigraphic unit B). If the glacier has a positive mass balance sufficiently high to maintain its front in this position, the ice-contact submarine fan will aggrade to the sea level and turn into a proglacial delta. But if the ice-front decouples itself from the moraine ridge and thereby loses the shoal's support, the glacier begins to calve in a rapid or catastrophic manner, depending upon the water depth and geometry of the basin (Alley 1991).

The formation of the Kregnes ridge was related to the Younger Dryas glacier's advance from an unknown upfjord position. The fjord was deep, and we infer that the glacier advanced by recycling its ice-contact submarine fan (as suggested by unit A*d*, Fig. 15), thus reducing the local seafloor depth and eventually coming to a halt (as indicated by unit B, Fig. 15). If the ice-front sedimentary record were limited to these two units only, it would be difficult to determine whether the glacier had re-advanced due to some spontaneous erratic cause (see above) or a significant, regional climatic deterioration. However, the Kregnes record shows the development of an impressive proglacial delta (unit C, Fig. 15), which indicates an ice-front stillstand of at least several decades and implies a regional episode of pronounced climatic cooling.

The deep palaeofjord directly south of the Kregnes ridge shows no evidence of any significant accumulation of ice-contact deposits along the walls, which suggests that the glacier has retreated by rapid calving. The nearest record of another major stillstand is a moraine ridge near Midttømme, 25 km south of Kregnes, which is an ice-contact delta linked by Reite (1985) to the Hoklingen substage (10 300–10 400 BP) of the Younger Dryas ice-sheet (Fig. 1).

The five radiocarbon dates available from the Kregnes ridge (Table 1) are from marine fauna remains found in different parts the delta foreset and coeval shoreline deposits. The sample dates are reasonably consistent, except for the one showing a surprisingly young age of 9690 ± 70 BP, which we are inclined to disregard as unreliable. The Younger Dryas time was characterized by several ^{14}C plateaux (Björck *et al.* 1996) and a relatively high isotopic age of sea water (Bard *et al.* 1996), and the mollusc shells in a delta environment may have been variably affected by freshwater. If the youngest date is excluded and the standard errors of the measurements are considered, the dates would appear to have a minimum range of 95 years (10 380 to 10 285 BP), which is rather satisfactory – on account of the three ^{14}C plateaux that occurred between 10 400 and 9600 BP (Björck *et al.* 1996). The five dates jointly yield a mean of 10 208 ± 99 BP, and if the highest and the lowest value are excluded – the mean appears to be nearly the same, 10 276 ± 95 BP.

Therefore, we tentatively suggest that the Kregnes "moraine" ridge may actually represent the Hoklingen substage and that the ice-front position of this stage in Gauldalen may thus have to be moved 25 km to the north (see Fig. 1).

The retreat of the Younger Dryas ice-sheet is widely considered to have involved two major re-advances. The occurrence of as many as three Younger Dryas "moraines" in Gauldalen points to at least three major re-advances, which means that the ice-front stillstands may have been relatively short and the sedimentation very rapid. The deltaic nature of the Kregnes ridge and the younger Midtømme ridge to the south indicates glacier grounding in the deep fjord and thus phases of marked climatic cooling, whereas the older, non-deltaic Melhus ridge to the north may represent ice re-advance due to a brief phase of climatic deterioration.

Conclusions

The Kregnes "moraine" ridge in Gauldalen is a Gilbert-type delta deposited at a Younger Dryas glacier terminus in a fjord basin. The gravelly delta consists of a north-dipping foreset, up to 150 m thick, comprised of turbidites, debrisflow and debrisfall deposits. The bottomset consists of turbiditic sand and mud, whereas the topset, 2–3 m thick, is a braided-river alluvium with local beach deposits, matching the marine limit of 175 m a.s.l. The fluvial palaeotransport direction corresponds with the northward progradation of the delta.

The fjord-wide delta front had an extent of 3 km and prograded over a distance of 1.5 km, in probably less than a hundred years, with the delta toe climbing by *c.* 50 m against the fjord's rapidly aggrading muddy floor. This may imply a basin-floor aggradation rate in excess of 50 cm/yr. The rate of the delta front progradation was likely non-linear, increasing due to the basin shallowing, but the mean rate could be higher than of 15 m/yr. The thin topset has an erosive horizontal base and implies stable sea level. The delta was advancing through the alternating episodes of toe aggradation and progradation, related to the increases and decreases of the delta-slope gradient. Slope steepening led to intense sediment sloughing by chutes/gullies and occasional large-scale failures.

The fjord's wave fetch was low and the wave base was generally no deeper than 1.5–2 m, but storm waves occasionally reworked the delta front to a depth of 6 m, probably due to strong, fjord-parallel southward winds. Glacitectonic deformation was limited to the depositional system's upfjord end, where the ice-contact surface is represented by a prominent topographic escarpment.

Allostratigraphic analysis suggests that the proglacial system commenced its development as an ice-contact submarine fan, which suffered glacitectonic deformation, quickly aggraded to the sea surface and turned into an ice-contact delta. The latter vigorously prograded and evolved into the large proglacial delta. The development of the delta was terminated by the renewed ice-sheet retreat, probably by rapid calving. The abandoned "moraine" ridge, modified by marine processes, was emerged by the regional glacio-isostatic uplift and has been deeply dissected and extensively eroded by river Gaula.

The occurrence of as many as three Younger Dryas "moraines" in Gauldalen indicates that the retreating ice front showed at least three major re-advances and its stillstands may thus have been relatively short. The deltaic nature of the Kregnes ridge and the younger Midtømme ridge to the south indicates phases of marked climatic deterioration. It is less likely that the non-deltaic Melhus ridge to the north represents an analogous climatic change.

Based on the available radiocarbon dates, it is tentatively suggested that the Kregnes ridge may represent the Hoklingen substage and that the ice-front position of this substage in Gauldalen may have to be moved 25 km to the north.

Acknowledgements. – The present paper is a result of a field workshop organized by the Norwegian Research Group for Quaternary Sedimentology (NFKS) and sponsored by the Geological Survey of Norway (NGU). The authors wish to thank all the other participants for their contribution and stimulating field discussions. The manuscript was critically reviewed by R. B. Alley and D. I. Benn. The radiocarbon dating of samples was done by the radiological laboratories in Trondheim and Uppsala. Two previously unpublished dates were used with the kind permission of T. Moseid (Norwegian University of Science and Technology).

References

Alley, R. B. 1991: Sedimentary processes may cause fluctuations of tidewater glaciers. *Annals of Glaciology 15*, 119–124.

Alley, R. B., Blankenship, D. D., Rooney, S. T. & Bentley, C. R. 1987: Till beneath ice stream B; 4, A coupled ice-till flow model. *Journal of Geophysical Research 92*, 8931–8940.

Andersen, B. G., Lundqvist, J. & Saarnisto, M. 1995a: The Younger Dryas margin of the Scandinavian ice sheet – an introduction. *Quaternary International 28*, 145–146.

Andersen, B. G., Mangerud, J., Sørensen, R., Reite, A., Sveian, H., Thoresen, M. & Bergstrøm, B. 1995b: Younger Dryas ice-marginal deposits in Norway. *Quaternary International 28*, 147–169.

Bard, E., Arnold, M., Mangerud, J., Paterne, M., Labeyrie, L., Dupat, J., Méliéres, M.-A., Sønstegaard, E. & Duplessy, J. C. 1994: The North Atlantic atmosphere-sea surface ^{14}C gradient during the Younger Dryas climatic event. *Earth and Planetary Science Letters 126*, 275–287.

Benn, D. I. 1996: Subglacial and subaqueous processes near a glacier grounding line: sedimentological evidence from a former ice-dammed lake, Achnasheen, Scotland. *Boreas 25*, 23–36.

Björck, S., Kromer, B., Johnsen, S., Bennike, O., Hammarlund, D., Lemdahl, G., Possnert, G., Lander Rasmussen, T., Wohlfarth, B., Hammer, C. U. & Spurk, M. 1996: Synchronized terrestrial-atmospheric deglacial records around the North Atlantic. *Science 274*, 1155–1160.

Blikra, L. H. & Longva, O. 1995: Frost-shattered debris facies of

Younger Dryas age in the coastal sedimentary successions in western Norway: palaeoenvironmental implications. *Palaeogeography, Palaeoclimatology and Palaeoecology 18*, 89–110.

Blikra, L. H. & Nemec, W. 1998: Postglacial colluvium in western Norway: depositional processes, facies and palaeoclimatic record. *Sedimentology 45*, 909–959.

Boulton, G. S. 1986: Push-moraines and glacier contact fans in marine and terrestrial environments. *Sedimentology 33*, 677–698.

Bornhold, B. D. & Prior, D. B. 1990: Morphology and sedimentary processes of the subaqueous Noeick River delta, British Columbia, Canada. *In* Colella, A. & Prior, D. B. (eds.): Coarse-Grained Deltas. *International Association of Sedimentologists Special Publication 10*, 169–181.

Colella, A. 1988: Pliocene–Holocene fan deltas and braid deltas in the Crati Basin, southern Italy: a consequence of varying tectonic conditions. *In* Nemec, W. & Steel, R. J. (eds.): *Fan Deltas: Sedimentology and Tectonic Settings*, 50–74. Blackie & Son, London.

Collinson, J. D. 1970: Bed forms of the Tana river, Norway. *Geografiska Annaler 52A*, 31–55.

Hampton, M. A. 1972: The role of subaqueous debris flows in generating turbidity currents. *Journal of Sedimentary Petrology 42*, 775–793.

Jopling, A. V. 1965: Hydraulic factors controlling the shape of laminae in laboratory deltas. *Journal of Sedimentary petrology 35*, 777–791.

Lowe, D. R. 1982: Sediment gravity flows: II. Depositional models with special reference to the deposits of high-density turbidity currents. *Journal of Sedimentary Petrology 52*, 279–297.

Lundqvist, J. & Saarnisto, M. 1995: Summary of project IGCP-253. *In* Lundqvist, J, Saarnisto, M. & Rutter, N. (eds.): IGCP 253, Termination of the Pleistocene – Final Report. *Quaternary International 28*, 9–18.

Lundqvist, J., Saarnisto, M. & Rutter, N. (eds.) 1995: IGCP 253, Termination of the Pleistocene – Final Report. *Quaternary International 2*, 201 pp.

Lønne, I. 1993: Physical signatures of ice advance in a Younger Dryas ice-contact delta, Troms, northern Norway: implications for glacier-terminus history. *Boreas 22*, 59–70.

Lønne, I. 1995: Sedimentary facies and depositional architecture of ice-contact glaciomarine systems. *In* Chough, S. K. & Orton, G. J. (eds.): Fan Deltas: Depositional Styles and Controls. *Sedimentary Geology 98*, 13–43.

Lønne, I. 1997a: Facies characteristics of a proglacial turbiditic sand-lobe at Svalbard. *Sedimentary Geology 109*, 13–35.

Lønne, I. 1997b: Sedimentology and depositional history of an early Holocene ice-contact submarine fan: the Egge-Lyngås "end-moraine", southern Norway. *Norsk Geologisk Tidsskrift 77*, 1–20.

Lønne, I. & Syvitski, J. P. 1997: Effects of the readvance of an ice margin on the seismic character of the underlying sediment. *In* Syvitski, J. P., Cooper, A. K. & Stoker, M. S. (eds.): COLDSEIS (Seismic Facies of Glacigenic Deposits). *Marine Geology 143*, 81–102.

Mann, D. H. 1986: Reliability of fjord glacier's fluctuations for paleoclimatic reconstructions. *Quaternary Research 25*, 10–24.

Massari, F. & Parea, G. C. 1988: Progradational gravel beach sequences in a moderate- to high-energy, microtidal marine environment. *Sedimentology 35*, 881–915.

Meier, M. F. & Post, A. 1987: Fast tidewater glaciers. *Journal of Geophysical Research 92 (B9)*, 9051–9058.

Naylor, N. A. 1980: The origin of inverse grading in muddy debris flow deposits – a review. *Journal of Sedimentary Petrology 50*, 1111–1116.

Nemec, W. 1990: Aspects of sediment movement on steep delta slopes. *In* Colella, A. & Prior, D. B. (eds.): Coarse-Grained Deltas. *International Association of Sedimentologists Spec Publication 10*, 29–73.

Nemec, W. 1995: The dynamics of deltaic suspension plumes. Oti, M. N. & Postma, G. (eds.): *The Geology of Deltas*, 31–9 Balkema, Rotterdam.

Nemec, W. & Steel, R. J. (eds.) 1988: *Fan Deltas: Sedimentolo and Tectonic Settings*. 444 pp. Blackie & Son, London.

Nemec, W., Steel, R. J., Gjelberg, J., Collinson, J. D., Prestholm E. & Øxnevad, I. E. 1988: Anatomy of collapsed and re-estab lished delta front in Lower Cretaceous of eastern Spitsberge gravitational sliding and sedimentation processes. *American Association of Petroleum Geologists Bulletin 72*, 454–476.

Postma, G. & Cruickshank, C. 1988: Sedimentology of a la Weichselian to Holocene terraced fan delta, Varangerfjord northern Norway. *In* Nemec, W. & Steel, R. J. (eds.): *Fan Deltas: Sedimentology and Tectonic Settings*, 144–157. Blackie & Son, London.

Postma, G. & Nemec, W. 1990: Regressive and transgressive sequences in a raised Holocene gravelly beach, southwestern Crete. *Sedimentology 37*, 907–920.

Postma, G., Nemec, W. & Kleinspehn, K. L. 1988: Large floating clasts in turbidites: a mechanism for their emplacement. *Sedimentary Geology 58*, 47–61.

Powell, R. D. 1981: A model for sedimentation by tidewater glaciers. *Annals of Glaciology 2*, 129–134.

Powell, R. D. 1991: Grounding line systems as second order controls on fluctuations of tidewater termini. *In* Anderson, J. B. & Ashley, G. M. (eds.): Glacial Marine Sedimentation: Paleoclimatic Significance. *Geological Society of America Special Paper 261*, 75–93.

Prior, D. B., Wiseman, W. J. & Bryand, W. R. 1981: Submarine chutes on the slope of fjord deltas. *Nature 290*, 326–328.

Prior, D. B. & Bornhold, B. D. 1988: Submarine morphology and processes of fjord fan deltas and related high-gradient systems: modern examples from British Columbia. *In* Nemec, W. & Steel, R. J. (eds.): *Fan Deltas: Sedimentology and Tectonic Settings*, 125–143. Blackie & Son, London.

Prior, D. B. & Bornhold, B. D. 1990: The underwater development of Holocene fan deltas. *In* Colella, A. & Prior, D. B. (eds.): Coarse-Grained Deltas. *International Association of Sedimentologists Special Publication 10*, 75–90.

Reite, A. J. 1983: Trondheim 1621 IV – kvartærgeologisk kart med beskrivelse, 1:50000. *Norges Geologiske Undersøkelse Skrifter 46*, 44.

Reite, A. J. 1985: Støren 1621 III – kvartærgeologisk kart med beskrivelse, 1:50000. *Norges Geologiske Undersøkelse Skrifter 65*, 25.

Reite, A. J. 1994: Weichselian and Holocene geology of Sør Trøndelag and adjacent parts of Nord Trøndelag county, central Norway. *Norges Geologiske Undersøkelse Bulletin 426*, 1–29.

Solheim, A. 1991: The depositional environment of surging subpolar tidewater glaciers. *Norsk Polarinstitutt Skrifter 194*, 97 pp.

Syvitski, J. P. M., Burrell, D. C. & Skei, J. M. 1987: *Fjords – Processes and Products*. 379 pp. Springer, New York, NY.

Walker, R. G. 1975: Conglomerates: sedimentary structures and facies models. *In* Harms, J. C., Walker, R. G. & Spearing, D. (eds.): Depositional Environments as Interpreted from Primary Sedimentary Structures and Stratification Sequences. *SEPM Short Course Lecture Notes 12*, 133–161.

Walker, R. G. 1992: Facies models and modern stratigraphic concept. *In* Walker, R. G. & James, N. P. (eds.): *Facies Models: Response to Sea Level Changes*, 1–14. Geological Association of Canada, St. John's.

Wolff, F. C. 1979: Beskrivelse til de berggrunnsgeologiske kart Trondheim og Østersund, 1:250000. *Norges Geologiske Undersøkelse 353*, 1–76.